1-1-2002

Titanium dioxide photocatalytic degradation of organophosphonates

Yun Bao
Iowa State University

Titanium dioxide photocatalytic degradation of organophosphonates

by

Yun Bao

A thesis submitted to the graduate faculty

in partial fulfillment of the requirements for the degree of

MASTER OF SCIENCE

Major: Organic Chemistry

Program of Study Committee:
William S. Jenks, Major Professor
Richard C. Larock
Jacob W. Petrich

Iowa State University

Ames, Iowa

2002

Graduate College
Iowa State University

This is to certify that the master's thesis of

Yun Bao

has met the thesis requirements of Iowa State University

Signatures have been redacted for privacy

TABLE OF CONTENTS

CHAPTER 1. BACKGROUND AND GENERAL THEORIES 1

1.1. Introduction 1

1.2. Brief introduction of various advanced oxidation processes (AOPs) 2

1.2.1. H_2O_2/UV process 2

1.2.2. Ozone/UV process 3

1.2.3. Photo-Fenton Reaction 3

1.2.4. Sonolysis 4

1.2.5. Radiolysis 4

1.2.6. Semiconductor-based photocatalysis 5

1.3. Semiconductor photocatalysis 6

1.3.1. Introduction 6

1.3.2. Chemical mechanism of initial steps 6

1.3.3. The nature of the oxidizing species (HO• radical vs hole) 7

1.3.4. Kinetic view 9

1.3.5. Some effects on the TiO_2 photocatalytic degradation process 10

1.3.5.1. Adsorption effect 10

1.3.5.2. Effect of pH 11

1.3.5.3. The effect of the amount of TiO_2 12

1.3.5.4. The effect of the concentration of the substrate 12

1.3.5.5. The effect of the concentration of the oxygen 13

1.3.5.6. The effect of reaction temperature 13

1.3.6. Application of TiO_2 photocatalysis 14

1.4. The objective and outline of this thesis 14

References 16

CHAPTER 2. TiO_2 PHOTOCATALYTIC DEGRADATION OF ORGANOPHOSPHONATES 21

2.1. Introduction 21

2.2. Experimental 23
2.2.1. Materials 23
2.2.2. General instrumentation 25
2.2.3. Preparation 25
2.2.4. Degradation procedures 31
2.3. Results 32
2.3.1. Control experiments 32
2.3.2. Photodegradation of DMPP 32
2.3.3. Effect of initial pH value on the photocatalytic degradation 35
2.3.4. Effect of initial concentration on the photocatalytic degradation 36
2.3.5. Effect of substituents of the phenyl on photocatalytic degradation 37
2.3.6. Study of the isotope effect by a competition reaction 40
2.3.7. Study of the photocatalytic degradation of ^{18}O-labeled DMPP 42
2.4. Discussion 45
2.4.1. Effect of initial pH and concentration 45
2.4.2. Degradation consistent with HO• radical chemistry 46
2.4.3. Mechanism study 47
2.5. Summary 47
References 49

APPENDIX 51

ACKNOWLEDGMENTS 59

CHAPTER 1. BACKGROUND AND GENERAL THEORIES

1.1 Introduction

The large production of chemicals has advanced the welfare of society. Unfortunately, the development of industry also brings pollution. It is important for us to realize the urgency to protect the environment for this generation and future generations. Drinking water is a basic necessity for people. Pesticide contamination and other chemical contamination force us to face up to the challenge of water purification. Treatment of contaminated surface water and groundwater, as well as wastewater, is part of a long-term strategy to improve the quality of our drinking water resources by elimination of toxic materials. Water purification is very important for the treatment of waste water to be used in industry, as well for obtaining the high-purity water needed for a number of industries, such as semiconductor device manufacturing, microelectronics, pharmaceuticals and electric power generation.

Photochemical processes are valuable techniques for water purification. Fundamental and applied research on this subject has been performed extensively during the last 20 years all over the world. Direct photochemical processes require an artificial light source, such as a high pressure mercury or a xenon arc lamp, and it requires a long time to decompose the organic compounds. In order to overcome the shortcomings, the combination of UV irradiation and other oxidizing agents has been considered, which has led to the development of Advanced Oxidation Processes (AOPs).[1]

AOPs include thermal processes with H_2O_2 or ozone, UV/H_2O_2 photolysis, UV/ozone photolysis, the photo-Fenton process, semiconductor-based photocatalysis, sonolysis, radiolysis and indirect electrolysis, etc.[2] The AOPs such as UV/H_2O_2, UV/ozone , and photo-Fenton processes, have already proven useful for carrying out the mineralization of organic compounds.[1,3,4] Other AOPs, such as semiconductor-based photocatalysis, sonolysis, and radiolysis, have also emerged as viable processes in recent years.[5-9] Although extensive research has been performed on semiconductor-based photocatalysis, there are still many mysteries in the chemistries and mechanisms of semiconductor-based photocatalysis

processes. The photodegradation reactions of organic pollutants may take place through the formation of harmful intermediates that are more toxic than the original compounds. Moreover, it is an important fundamental question to understand the mechanisms of the oxidative chemistry. Identification of the intermediates serves both interests. The intermediates of the TiO_2 photocatalytic degradation of dimethyl phenylphosphonate, chosen as a model for organophosphonates in general, has been investigated in this research.

Organophosphonates, many of which are hazardous pesticides and chemical warfare agents, can be very toxic and harmful. Dimethyl phenylphosphonate has similar structural features to these pesticides and chemical warfare agents but is less toxic. It can serve as a model compound to study the chemistry at phosphorus. Only a few articles have been published the TiO_2 photocatalytic degradation of organophosphonates, but the chemistry and mechanisms of degradation have not been clarified.[10,11] Using dimethyl phenylphosphonate as a model, the TiO_2 semiconductor-based photodegradation process will be reported in this thesis. Other AOPs may be mentioned or investigated as the compared methods. In this chapter, some basic concepts of AOPs are presented, followed by a detailed discussion of the TiO_2-induced photodegradation process.

Scheme 1.1. Structure of pesticide, nerve agent

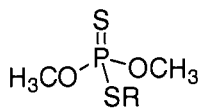

R = $CH(CO_2Et)CH_2CO_2Et$

Malathion

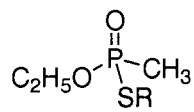

R = $CH_2CH_2N(i\text{-}Pr)_2$

VX

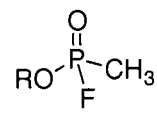

R = *i*-Pr; GB (Sarin)

R = C_6H_{13}; GD (Soman)

1.2. A brief introduction to various Advanced Oxidation Processes (AOPs)

1.2.1. H_2O_2/UV process

Hydroxyl radical can be generated in the photolysis of hydrogen peroxide (equation 1.1).

$$H_2O_2 \xrightarrow{h\nu} 2\,HO\cdot \qquad (1.1)$$

Hydroxyl radicals can react with hydrogen peroxide to generate hydroperoxyl radical, which is also an oxidizing reagent (equation 1.2).

$$H_2O_2 + HO\bullet \longrightarrow H_2O + HOO\bullet \qquad (1.2)$$

After generation of the hydroxyl radicals, they can further react with organic substrates by hydrogen abstraction, electrophilic addition and electron transfer mechanisms. There is wide research on the utilization of the H_2O_2/UV oxidation process to remove toxic organic pollutants.[1,12-15] The advantages of this process include the fact that hydrogen peroxide is a cheap and easy to handle oxidant, infinitely miscible with water. However, the absorption coefficient of hydrogen peroxide and the quantum efficiency of hydroxyl radical production is very low at $\lambda > 250$ nm.[1] Moreover, the hydrogen peroxide has to be gotten rid of after the reaction.

1.2.2. Ozone/UV process

The high standard redox potential of ozone (2.07 V at pH = 1) makes ozone a powerful oxidant useful for the degradation of organic pollutants in water.[16,17] Additionally, the ozone/UV process generates HO• radicals by the light-induced homolysis of O_3 and subsequent interaction of $O(^1D)$ with water (equation 1.3).[18]

$$O_3 \xrightarrow{h\nu < 310\ nm} O_2 + O(^1D)$$
$$O(^1D) + H_2O \longrightarrow HO\bullet + HO\bullet \qquad (1.3)$$

A second explanation for production of the hydroxyl radical in the photolysis of ozone dissolved in water involves the formation of H_2O_2 (equation 1.4), since hydrogen peroxide has been observed during the photolysis of ozone dissolved in water. The resulting H_2O_2 is then a source of HO• radicals via photohomolysis. The disadvantage of this ozone/UV process is the expensive production of ozone.

$$O_3 + H_2O \xrightarrow{h\nu} H_2O_2 + O_2 \qquad (1.4)$$

1.2.3. Photo-Fenton Reaction

The Fenton reagent Fe^{2+} is a well-known oxidant, generating an hydroxyl radical as shown by the following equation (equation 1.5).[19]

$$Fe^{2+} + H_2O_2 \longrightarrow Fe^{3+} + HO^- + HO\bullet \quad (1.5)$$

The Fenton reagent has been applied to both water and soil treatment. Furthermore it was found that a more effective system for oxidative degradation can be realized by applying near UV/Vis irradiation to the basic Fenton reaction (equation 1.6).[4,20,21] Usually complete degradation can be realized in a short period during the photo-Fenton process. However, the iron salts constitute a pollution source and they must be removed. Since the reaction takes place at pH 2-3, neutralization is necessary to precipitate the dissolved iron as $Fe(OH)_3$.

$$Fe^{2+} + H_2O + h\nu \longrightarrow Fe^{3+} + H^+ + HO\bullet \quad (1.6)$$

1.2.4. Sonolysis

Sonochemical degradation methods are relatively new and involve acoustic cavitation, the cyclical growth and collapse of gas bubbles.[22] Propagation of an ultrasound wave in aqueous solution leads to the formation of cavitation bubbles. The collapse of these bubbles spawns extreme conditions on the microscopic scale, such as very high temperatures and pressures, which in turn lead to the dissociation of H_2O and the production of radical species, such as HO•, HOO•, etc. These can be subsequently used for the transformation and/or destruction of organic substrates. Evidence has accumulated indicating that higher ultrasound frequencies at ~400 KHz are more favorable for the production of HO• radicals.[23] The O'Shea group[7,11] has used sonolysis to decompose hazardous organophosphorus compounds to CO_2, H_2O and H_3PO_4.

1.2.5. Radiolysis

Radiolysis refers to bond cleavage or any chemical process brought about by high-energy radiation.[24] The decay of radioactive nuclei (α, β, and γ radiation), a beam of accelerated charged particles (electrons, protons, deuterons, helium and heavier nuclei), and short-wavelength radiation (X or Bremsstrahlung radiation) are the most commonly used as the types of radiation for the radiolysis process.

Organic contaminants in aqueous solutions can be destroyed either by a "direct" or "indirect" interaction with the incident radiation. Because of the low concentration of

organic contaminants in aqueous solution, the decomposition of organic contaminant takes place by "indirect" radiolysis, i.e. by interacting with e^-_{aq}, H•, and HO• and the hydrogen peroxide generated by radiation-induced reaction with the water (equation 1.7):[25]

$$H_2O \xrightarrow{\text{radiation}} [2.6]\, e^-_{aq} + [0.6]\, H\bullet + [2.7] HO\bullet + [0.7]\, H_2O_2 + [2.6]\, H_3O^+ + [0.45]\, H_2 \quad (1.7)$$

The number in brackets is the radiation chemical yield (G value), defined as the number of species generated per 100 eV of absorbed energy or the approximate micromolar concentration per 10 J of absorbed energy.[25]

1.2.6. Semiconductor-based photocatalysis

Mineralization of organic pollutants in water and air steams to CO_2, H_2O and inorganic ions can be realized by using certain semiconductors as photocatalysts. [1,2,5,26-30] There are a lot of different semiconductor materials which are readily available, but only a few are suitable for photodegradation of organic pollutants, namely, WO_3, TiO_2, $SrTiO_3$, CdSe, CdTe, ZnO, CdS and ZnS. In order to make a semiconductor suitable for mineralizing organic waste products, the redox potential of the photogenerated valence band hole must be sufficiently positive to generate adsorbed HO• radical, and the redox potential of the photogenerated conduction band electron must be sufficiently negative to be able to reduce absorbed O_2 to superoxide.[31] Of all the different semiconductor photocatalysts, TiO_2 seems to be the most active.[32] In addition, TiO_2 is very cheap catalyst and can be recycled. Furthermore, the suspended photocatalyst TiO_2 is stable to the photolysis conditions and a large number of oxidative conversions per active site on the catalyst can be attained without significant degradation of the semiconductor's redox catalytic capacity. Thus, TiO_2 photocatalysis is becoming an active field of research and commercial interest. In section 1.3, TiO_2-based photolysis will be discussed in detail.

1.3. Semiconductor photocatalysis

1.3.1. Introduction

TiO_2 is considered a promising photodegradation catalysis because it possesses five basic characteristics: 1) photoactive, 2) able to utilize near UV-light, 3) biologically and chemically inert, 4) photostable, and 5) inexpensive.[33] In order to improve the reproducibility of the results between groups, many have chosen to use a particular source of TiO_2, Degussa P25, produced through the high temperature (greater than 1200 °C) flame hydrolysis of $TiCl_4$ in the presence of hydrogen and oxygen, which continues to be treated with steam to remove HCl. The two crystal structures of TiO_2 usually utilized in photocatalysis are rutile and anatase. Degussa P25 is approximately 70% anatase and 30% rutile. This brand TiO_2 was used in this study. In order to gain insight into the TiO_2 photodegradation, the initial events of the TiO_2 photocatalytic system are going to be discussed first.

1.3.2. The chemical mechanism of the initial steps[5]

Typical photodegradation is performed with oxygen- or air-saturated aqueous suspensions of TiO_2 (Degussa P25). The energy band gap of anatase is 3.23 eV (384 nm) and rutile is 3.02 eV (411 nm).[34] The band gap of Degussa P25 is roughly 3.2 eV.[35] When ultraviolet radiation equaling or exceeding the energy of the bandgap (<400 nm) is absorbed, an electron is promoted from the valence band to the conduction band leaving an electron hole (h_{VB}^+) in the valence band. This process is shown in equation 1.8.

$$TiO_2 + h\nu \longrightarrow e^-_{cb} + h^+_{vb} \quad (1.8)$$

$$H_2O_{ads} + h^+_{vb} \longrightarrow HO\bullet_{ads} + H^+ \quad (1.9)$$

$$O_2 + e^-_{cb} \longrightarrow O_2^{\bullet -} \quad (1.10)$$

$$O_2^{\bullet -} + H^+ \longrightarrow HO_2\bullet \quad (1.11)$$

$$2HO_2\bullet \longrightarrow H_2O_2 + O_2 \quad (1.12)$$

$$H_2O_2 + e^-_{cb} \longrightarrow HO\bullet_{ads} + HO^- \quad (1.13)$$

$$A + e^-_{cb} \longrightarrow A^{\bullet -} \quad (1.14)$$

$$D + h^+_{vb} \longrightarrow D^{\bullet +} \quad (1.15)$$

Adsorbed water on the surface of the TiO_2 can continue to react with the hole to generate the hydroxyl radical as shown in equation 1.9. This process is the main mode for adsorbed hydroxyl radical formation. Hydroxyl radicals are believed to be the main oxidation reagents during TiO_2 photocatalytic degradation and it is assumed that the reactions take place on the TiO_2 surface, but electron transfer is another important mechanism.[6,36-45] Photocatalytic degradations are carried out in aqueous solution and with oxygen. The main role of the oxygen is as an electron consumer reacting with a conduction band electron to form superoxide as seen in equation 1.10 and preventing electron-hole recombination.[46] Superoxide, by subsequent reactions, can form hydroperoxyl radical and hydrogen peroxide, shown in steps 1.11 and 1.12, respectively. Evidence for the formation of hydroperoxyl radical has also been reported.[45] Hydrogen peroxide may then undergo fragmentation to an hydroxyl radical and an hydroxide anion, as seen in equation 1.13.

It has also been reported that organic molecules may interact directly with an electron in the conduction band or an electron hole in the valence band.[41] These steps are represented in equations 1.14 and 1.15. The symbol A represents a general electron acceptor molecule while D signifies an electron donor molecule. Of course, there exists an important charge and hole recombination reaction in the initial steps.

The results of detailed laser flash photolysis experiments have indicated the characteristic time scales of the processes associated with the reaction mechanism.[5] The charge-carrier generation (equation 1.8) occurs on the femtosecond time scale. Charge carrier trapping (equation 1.9) occurs on a picosecond to nanosecond time scale. The charge-carrier recombination is on the picosecond to nanosecond time scale, while the interfacial charge transfer is on a microsecond to millisecond time scale.

1.3.3. The nature of the oxidizing species ($HO_{ads}\bullet$ radical vs hole)

In aqueous solution, two main oxidizing species are proposed in TiO_2 photocatalytic degradation process, the hydroxyl radical or the irradiation-induced hole. It has been

suggested by a radiolytic study that the surface-trapped hole, which they distinguish from a deep hole, and a surface-bound hydroxyl radical are indistinguishable species.[42] There exists a significant body of literature that oxidation may occur by either indirect oxidation via the hydroxyl radical or directly by a valence-band hole.[6,36-45]

Chemical evidence in support of HO• radical as the principal reactive oxidant in photoactivated TiO_2 is the observation of hydroxylated intermediates during the photocatalytic degradation of aromatic compounds. When those compounds react with a known source of hydroxyl radicals, similar intermediates are produced as those in the photocatalytic degradation processes. For example, Jenks et al.[47] studied the decomposition of anisole by using photoactivated TiO_2 system, direct H_2O_2/UV system and the Fenton system. The distribution of the intermediates observed in the different systems is similar; *para*- and *ortho*-hydroxy anisole are the main intermediates. This phenomenon is consistent with the hydroxyl radical being the main oxidation reagent during the primary photodegradation of anisole. In addition, ESR studies[48] and indirect kinetic evidence[49] have verified the existence of hydroxyl radicals in aqueous solutions of illuminated TiO_2.

However, product identification does not always permit a delineation of HO• versus hole oxidation, since the hydroxylated products can originate by direct hole oxidation to give the cation radical which subsequently undergoes hydration in the solvent water. Jenks et al.[50,51] have suggested that the ring-opening on TiO_2 photocatalytic degradation of 4-chlorophenol was induced by direct single electron transfer, rather than hydroxyl radical reaction. Mao et al[52] have observed that trichloroacetic acid and oxalic acid are oxidized primarily by valence-band hole on TiO_2 via a photo-Kolbe process. Likewise, Draper and Fox[39] were unable to find evidence of any hydroxyl radical adducts for the aqueous TiO_2-sensitized reaction of potassium iodide, etc. They observed only the products of the direct electron-transfer oxidation. Carraway et al.[53] have provided experimental evidence for the direct hole oxidation of tightly bound electron donors, such as formate, acetate, and glyoxylate, at the semiconductor surface.

Richard[54] has argued that both holes and hydroxyl radicals are involved in the photooxidation of 4-hydroxybenzyl alcohol (HBA) on ZnO or TiO_2. His results suggest positive holes and hydroxyl radicals have different regioselectivities in the photocatalytic

transformation of HBA. Hydroquinone (HQ) is thought to result mainly from the direct oxidation of HBA by h_{vb}^+, dihydroxybenzyl alcohol (DHBA) mainly from reaction with hydroxyl radical, while 4-hydroxybenzaldehyde (HBZ) is produced by both pathways. In the presence of isopropyl alcohol, which is used as a hydroxyl radical quencher, the formation of DHBA is completely inhibited and the formation of HBZ is inhibited.

1.3.4. Kinetic view

In general, the kinetics of TiO_2 photomineralization of organic substrates in the presence of oxygen and under steady state illumination fit a Langmuir-Hinshelwood kinetic scheme. The Langmuir-Hinshelwood equation is derived from a model in which the organic reagent is pre-adsorbed on the photocatalyst surface prior to UV illumination. The rate of degradation is proportional to the surface coverage (θ) (equation 1.16).[49]

$$\text{Rate} = k\,\theta \tag{1.16}$$

After writing out the formulation of θ, the above equation can be converted into the common Langmuir-Hinshelwood kinetic model (equation 1.17), where k_{obs} is an apparent reaction rate constant and K_L is the Langmuir constant reflecting the adsorption/desorption equilibrium between the reagent and the surface of the photocatalyst.

$$\frac{dC}{dt} = \frac{k_{obs}K_L C}{(K_L C + 1)} \tag{1.17}$$

There are two extreme cases. For a high concentration of the pollutant, where saturation coverage of the surface is achieved (i.e. $K_L C >> 1$), the equation can be simplified to a zero-order rate equation (equation 1.18).

$$\frac{dC}{dt} = k_{obs} \tag{1.18}$$

For a low concentration ($K_L C << 1$), the equation can be simplified to a pseudo-first-order kinetic equation (equation 1.19).

$$\frac{dC}{dt} = k_{obs}K_L C \tag{1.19}$$

Considering that the solvent and reaction intermediates compete with the reacting substrate for the active surface, the Langmuir-Hinshelwood kinetic model can be characterized by equation (equation 1.20):

$$\frac{dC}{dt} = \frac{k_{obs}K_L C}{(K_L C + \sum K_i C_i + 1)} \tag{1.20}$$

where K_iC_i are adsorption constants and concentrations of competitively adsorbed species. When the concentration of the reacting substrate is high, this equation can be similarly transferred into the zero-order equation.

When the concentration of the reacting substrate is low, the Langmuir-Hinshelwood equation is converted into its inverse function, resulting in a linear relationship with an intercept of k_{obs}^{-1} and a slope of ($k_{obs}^{-1}K^{-1}$) (equation 1.21).

$$\frac{dt}{dC} = \frac{1}{k_{obs}} + \frac{1}{k_{obs}K_L C} \tag{1.21}$$

The process in which a surface-generated catalytic species diffuses to the bulk solution where the primary catalytic conversion occurs can be described by an Eley-Rideal pathway.[55] Turchi and Ollis[49] have shown that the rate of photo-oxidation of an organic substrate in the bulk solution with the oxidative species diffused from irradiated TiO_2 presents the same kinetic behavior as the Langmuir-Hinshelwood kinetic model. Unfortunately, an experimental distinction between the Langmuir-Hinshelwood kinetic model and Eley-Rideal pathway, based on kinetics alone, is not possible, because of the kinetic ambiguities.[56,57] The kinetic expression can be the same irrespective of (1) the oxidizing species and the substrate are both adsorbed, (2) both species are in solution, (3) the oxidizing species is adsorbed and the substrate is in solution, or (4) the substrate is adsorbed and the oxidant is in solution.

1.3.5. Some effects on the TiO_2 photocatalytic degradation process

1.3.5.1. Adsorption effect

It has been suggested that preliminary adsorption is a prerequisite for highly efficient detoxification.[58] Because recombination of the photogenerated electron and hole is so rapid, interfacial electron transfer is kinetically competitive only when the relevant donor or acceptor is preadsorbed before photolysis, thus efficient conversion of the adsorbed photon to a chemically stored redox equivalent is to be achieved. The strong correlation between

degradation rates and concentration of the organic pollutant adsorbed to the surface also implies that the hydroxyl radicals or trapped holes are directly available at the surface.[59-61]

Our group has studied the photodegradation of 4-chlorophenol.[50,51] An interesting result is that ring opening easily happens until there are two hydroxyl groups in the *ortho* position on the phenyl ring. This result may be explained in that two *ortho* hydroxyl groups can anchor the substrate on the TiO_2 surface. Then, the substrate can react with a hole to generate the radical species further reacting with the superoxide to occur the ring opening. The adsorption phenomenon involving in anisole is investigated.[62] Isopropyl alcohol was used as a competitive absorption substrate that can compete with the weaker absorbed species on TiO_2. When there are more methoxy groups on the ring, the rate inhibition effects of isopropanol are more obvious, while more hydroxyl group substitutents on phenyl ring, the effect of isopropanol is less obvious.

1.3.5.2. Effect of pH

The particle size, surface charge and band edge positions of TiO_2 are strongly influenced by pH. The isoelectric point for TiO_2 in water is about pH = 6.6,[63] and positive surface charge is expected at lower pH and negative surface charge is predicted at higher pH values. This surface charge is due to protonation or deprotonation of the surface HO groups. A second charge layer is formed in the electrolyte near the interface in response to the surface charge (see Figure 1.1). For negative charges accumulated at the interface of n-type semiconductor, the space charge layer formed is a depletion layer and the bands bend upward toward the surface (see Figure 1.1 c). Thus, the concentration of holes on the surface is larger than that of electrons. The higher concentration holes may react with a high concentration of HO^- on the suface.[6] Therefore, a higher concentration of hydroxyl radical is produced. However, the change in the rate of photocatalytic degradation rate is generally less than one order of magnitude from pH 2 to pH 12 and evidence for higher reaction rates for various photocatalytic degradations at both low pH or at high pH can be found in the literature.[64-67]

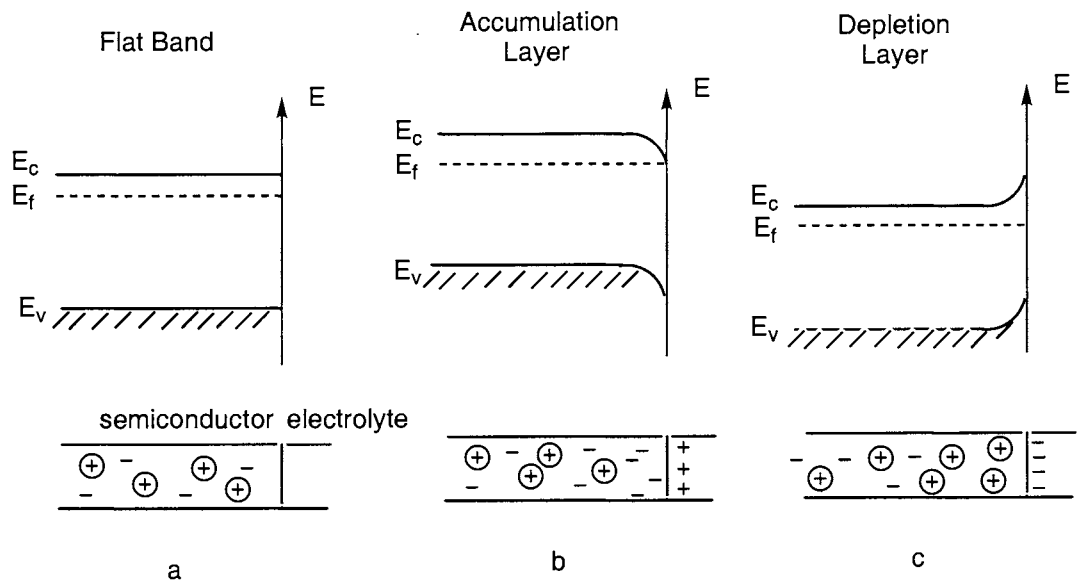

Figure 1.1. Space charge layer formation and band bending for n-type semiconductor-solution interface (E_c: conduction band potential energy; E_v: valence band potential energy; E_f: Fermi level energy): a. shows the flat band potential diagram in the absence of a space charge layer; b. pH < 6.6., accumulation layer at the present of a positive charge on the surface; c. pH > 6.6, depletion layer at the presence of a negative charge on the surface.

1.3.5.3. The effect of the amount of TiO_2

Usually, the rate of reaction is almost linearly dependent on the increased concentration of TiO_2, and then gradually levels off.[68,69] This behavior is consistent with the complete absorption of light near the surface of the semiconductor.[68,69] In some cases, with the increased concentration of TiO_2, the rate of degradation increases up to a certain point, then begins to decrease slowly.[70,71] The reason is that when the amount of TiO_2 increases, there are more active sites for the reaction, thus the reaction rate increases. When the amount of TiO_2 is more than the optimum concentration, however, the aggregation of TiO_2 becomes a serious problem and the reaction rate slows. The increase in the opacity and light scattering by the particles may be the other reason for the decrease in the rate. In commercial systems, TiO_2 has been fixed on Nafion film, ceramic film, silica gel, and a glass surface.[72]

1.3.5.4. The effect of the concentration of the substrate

As discussed earlier in the section 1.3.4, the concentration of organic substrate affects the rate of the degradation. It is also clear that the kinetics of photodegradation will depend

on the ease with which the substrate can be oxidized and how well it absorbs and how well its products adsorb on the surface TiO_2. For most of the organic pollutants tested, the relationship of degradation rate and pollutant's concentration comply with the Langmuir-Hinshelwood kinetic model.[51,62] This is not always the fact. San et al.[71] during their study of TiO_2 photocatalytic degradation of nitrophenol found a decrease in the initial degradation rate with an increase in the initial concentration of nitrophenol, due to strong adsorption of the products. It is also worth noting that the absorption spectrum of the pollutant can drastically affect the kinetics of photocatalysis. In particular, if the pollutant is a strong UV absorber, then, as its concentration is increased it will eventually begin significantly to screen the TiO_2 and the rate of the degradation will be affected.

1.3.5.5. The effect of the concentration of the oxygen

Since oxygen is the electron consumer inhibiting the recombination of the electron/hole pair, the concentration of dissolved oxygen in solution also affect the degradation rate. It is found that the rate degradation is proportional to the fraction of O_2 (equation 1.22),[31] Where K_{O_2} is the Langmuir adsorption coefficient for O_2.

$$Rate \propto \frac{K_{O_2}[O_2]}{1+K_{O_2}[O_2]} \tag{1.22}$$

1.3.5.6. The effect of reaction temperature

Photochemical reactions are often not very temperature sensitive. The reactant is converted into product through an excited state surface funnel crossing an excited-state surface to a ground-state surface.[73] The overall process of TiO_2 photodegradation is only slightly temperature sensitive. The activation energies of photocatalytic degradation reactions usually have the values of 5 – 16 kJ mol^{-1},[31] because the photocatalytic degradation process involves potentially temperature-dependent steps, such as adsorption, desorption, surface migration, and rearrangement. In principle, it is possible to sort the temperature dependence into (1) adsorption contribution (by alteration of the Langmuir adsorption isotherm), (2) stabilization of intermediates (by alteration of kinetics for formation or decay of different transients), and (3) environmental effects (by variation of solvent, electrolytes, etc.).[74]

1.3.6. Application of TiO_2 photocatalysis

The semiconductor-sensitized photomineralization of organic substrate by oxygen can be summarized as follows (equation 1.23).

$$\text{Organic pollutant} + O_2 \xrightarrow[h\nu \geq E_{bg}]{TiO_2} CO_2 + H_2O + \text{Mineral acid} \qquad (1.23)$$

The degradation of a variety of organic molecules has been investigated. For an exhaustive review of these publications, please refer to Hoffman[5] and Mills.[33] Various examples of the photomineralization of organic pollutants by TiO_2 are summarized in Table 1. The research related to the degradation of organic compounds by photocatalysis has progressed rapidly. Mills suggests that it is necessary to define a standard test system.[31] 4-Chlorophenol has become a standard for evaluating various experimental parameters.[9,50,51,57,59,75-91]

1.4. The objective and outline of this thesis

The objective of my research is to study the chemistry and chemical mechanism of TiO_2 photocatalytic degradation of dimethyl phenylphosphonate (DMPP) in oxygen saturated aqueous solution as a model for other organophosphonates. The conditions which affect the photodegradation and the intermediates of the photodegradation will be investigated. From a mechanistic standpoint, we are interested in whether or not the chemistry is attributable to $HO\bullet_{ads}$ and, if so, whether alkyl degradation is initiated by attack at the alkyl center, the phosphorus, or both. In order to clarify the mechanism, deuterium and ^{18}O-labelled substrates will be synthesized and then degradation reactions will be investigated.

Table1.1. Photomineralization of organic pollutants by TiO_2: Examples of compounds[31]

Class	Examples
Alkanes	methane; isobutane; pentane; isooctane; heptane; *n*-dodecane; cyclohexane; methylcyclohexane; 1,4-methylcyclohexane; paraffin
Haloalkanes	mono-,di-, tri-, and tetrachloromethane; fluorotrichloromethane; 1,1- and 1,2-dichloroethane; tetrachloroethane, pentachloroethane; dibromoethane; tribromoethane; 1,2-dichloropropane; 1-bromododecane; 1,1-difluoro-1,2-dichloroethane; 1,1-difluoro-1,2,2-trichloroethane
Aliphatic alcohols	methanol; ethanol; isopropyl alcohol; cyclobutanol; *n*-propyl alcohol; propan-2-ol; butanol; penta1,4-diol; 2-ethoxyethanol; 2-butoxyethanol; dodecanol; benzyl alcohol; glucose; sucrose
Aliphatic carboxylic acids	formic; ethanoic; dimethylethanoic; mono-, di-, and tri-chloroethanoic; propanoic; butanoic; dodecanoic; oxalic
Alkenes	Propene; cyclohexene
Haloalkenes	tetrachloroethene; 1,2-dichloroethene; 1,1,1- and 1,1,2-trichloroethene; tetrachloroethene; mono-, di-, and tetra-fluoroethene; hexafluoropropene
Aromatics	Benzene; naphthalene
Haloaromatics	chlorobenzene; bromobenzene; 2,3,4-chlorophenol; 2,4- and 3,4-dichlorophenol; 2,4,5- and 2,4,6-trichlorophenol; pentachlorophenol; 2,3-, and 4-fluorophenol; 2,4- and 3,4-dichloronitrobenzene; 1,2-dichloro nitrobenzene
Phenols	phenol; hydroquinone; methylhydroquinone; catechol; 4-methylcatechol; 4-nitrocatechol; resorcinol; 2-naphthol; *o*-, *m*-, and *p*-cresol
Aromatic carboxylic acid	benzoic; 4-aminobenzoic; 3-chloro-4-hydroxybenzoic; phthalic; salicyclic; *m*-, and *p*-hydroxybenzoic; 3-chlorohydroxybenzoic acid
Polymers	polyethylene; PVC
Surfactants	SDS; *p*-nonyl phenyl polyoxyethylene ether; polyethylene glycol; *p*-nonyl phenyl ether; sodium dodecylbenzene sulfonate; benzyldodecyl dimethylammonium chloride; *p*-nonyl phenyl poly(oxyethylene)esters; sodium benzenesulfonate; paraxon; malathion; 4-nitrophenyl ethyl phosphinate; 4-nitrophenyl isopropyl phosphinate; 1-hydroxy ethane-1,1-diphosphonate; 4-nitrophenyl diethyl phosphate; trimethyl phosphate; trimethyl phosphite; dimethylammonium phosphodithionate; tetrabutylammonium phosphate
Herbicides	methyl viologen; atrazine; simazine; prometon; propetryne; bentazon
Pesticides	DDT; parathion; lindane
Dyes	methylene blue; rhodamine B; methyl orange; fluorescerin; umbelliferone

References:

(1) Legrini, O.; Oliveros, E.; Braun, A. M. *Chem. Rev.* **1993**, *93*, 671-698.

(2) Kamat, P. V.; Vinodgopal, K. In *Molecular and Supramolecular Photochemistry: Organic and Inorganic Photochemistry*; Ramamurthy, V., Schanze, K., Eds.; Marcel Dekker: New York, 1998; Vol. 2, p 307-350.

(3) Mill, T.; Gould, C. W. *Environ. Sci. Technol.* **1979**, *13*, 205.

(4) Bauer, R.; Fallmann, H. *Res. Chem. Intermed.* **1997**, *23*, 341-354.

(5) Hoffmann, M. R.; Martin, S. T.; Choi, W.; Bahnemann, D. W. *Chem. Rev.* **1995**, *95*, 69-96.

(6) Linsebigler, A. L.; Lu, G.; Yates, J. T., Jr. *Chem. Rev.* **1995**, *95*, 735-758.

(7) O'Shea, K. E.; Aguila, A.; Vinodgopal, L. K.; Kamat, P. V. *Res. Chem. Intermed.* **1998**, *24*, 695-705.

(8) Choure, S. C.; Bamatraf, M. M. M.; Rao, B. S. M.; Das, R.; Mohan, H.; Mittal, J. P. *J. Phys. Chem. A* **1997**, *101*, 9837-9845.

(9) Stafford, U.; Gray, K. A.; Kamat, P. V. *Chem. Oxid.* **1997**, *4*, 193-204.

(10) O'Shea, K. E.; Beightol, S.; Garcia, I.; Aguilar, M.; Kalen, D. V.; Cooper, W. J. *J. Photochem. Photobiol. A* **1997**, *107*, 221-226.

(11) O'Shea, K. E.; Garcia, I.; Aguilar, M. *Res. Chem. Intermed.* **1997**, *23*, 325-339.

(12) Soerensen, M.; Frimmel, F. H. *Z. Naturforsch., B: Chem. Sci.* **1995**, *50*, 1845-1853.

(13) Sorensen, M.; Frimmel, F. H. *Water Res.* **1997**, *31*, 2885-2891.

(14) Benitez, F. J.; Beltran-Heredia, J.; Acero, J. L. *Toxicol. Environ. Chem.* **1996**, *56*, 199-210.

(15) Stefan, M. I.; Hoy, A. R.; Bolton, J. R. *Environ. Sci. Technol.* **1996**, *30*, 2382-2390.

(16) Lelacheur, R. M.; Glaze, W. H. *Environ. Sci. Technol.* **1996**, *30*, 1072-1080.

(17) Hausler, R.; Briere, F. G.; Beron, P. *Ozone Sci. Eng.* **1993**, *15*.

(18) Peyton, G. R.; Glaze, W. H. *Environ. Sci. Technol.* **1988**, *22*, 761-767.

(19) Walling, C. *Acc. Chem. Res.* **1975**, *8*, 125-131.

(20) Zepp, R. G.; Faust, B. C.; Hoigné, J. *Environ. Sci. Technol.* **1992**, *26*, 313-319.

(21) Pignatello, J. J.; Sun, Y. *Water Res.* **1995**, *29*, 1837-1844.

(22) Johnston, A. J.; Hocking, P. *ACS Symp. Ser.* **1993**, *518*, 106-18.

(23) Suslick, K. S. *Ultrasound: Its Chemical, Physical and Biological Effects*; VCH Publ.: New York, 1988.

(24) Parmon, V.; Emeline, A. V.; Serpone, N. *Intern. J. Photoenergy* **2002**, *4*, 91-131.

(25) Buxton, G. V.; Greenstock, C. L.; Helman, W. P.; Ross, A. B. *J. Phys. Chem. Ref. Data* **1988**, *17*, 520.

(26) *Aquatic and Surface Photochemistry*; Helz, G. R.; Zepp, R. G.; Crosby, D. G., Eds.; Lewis Publishers: Boca Raton, 1994.

(27) *Photocatalytic Purification and Treatment of Water and Air*; Ollis, D. F.; Al-Ekabi, H., Eds.; Elsevier Science Publishers: New York, 1993.

(28) *Photocatalysis: Fundamentals and Applications*; Serpone, N.; Pelizzetti, E., Eds.; John Wiley & Sons: New York, 1989.

(29) Bahnemann, D. In *Handbook of Environmental Chemistry*; Boule, P., Ed.; Springer: Berlin, Germany, 1999; Vol. 2 L, p 285-351.

(30) Fujishima, A.; Hashimoto, K.; Watanabe, T. *TiO_2 Photocatalysis Fundamentals and Applications*; BKC, Inc.: Tokyo, 1999.

(31) Mills, A.; Davies, R. H.; Worsley, D. *Chem. Soc. Rev.* **1993**, *22*, 417-425.

(32) Barbeni, M.; Pramauro, E.; Pelizzetti, E.; Borgarello, E.; Serpone, N. *Chemosphere* **1985**, *14*, 195.

(33) Mills, A.; Le Hunte, S. *J. Photochem. Photobiol. A: Chem.* **1997**, *108*, 1-35.

(34) Rajeshwar, K. *J. Appl. Electrochem.* **1995**, *25*, 1067.

(35) Martin, S. T.; Herrmann, H.; Hoffmann, M. R. *J. Chem. Soc., Faraday Trans.* **1994**, *90*, 3323.

(36) Micic, O. I.; Zhang, Y.; Cromack, K. R.; Trifunac, A. D.; Thurnauer, M. S. *J. Phys. Chem* **1993**, 14284-13288.

(37) Micic, O. I.; Zhang, Y.; Cromack, K. R.; Trifunac, A. D.; Thurnauer, M. S. *J. Phys. Chem.* **1993**, *97*, 7277-7283.

(38) Howe, R. F.; Grätzel, M. *J. Phys. Chem.* **1987**, *91*, 3906-3909.

(39) Draper, R. B.; Fox, M. A. *Langmuir* **1990**, *6*, 1396-1402.

(40) Draper, R. B.; Fox, M. A. *J. Phys. Chem.* **1990**, *94*, 4628-4634.

(41) Fox, M. A. In *Photocatalytic Purification and Treatment of Water and Air*; Ollis, D. F., Al-Ekabi, H., Eds.; Elsevier: 1993; Vol. 3, p 163-167.

(42) Lawless, D.; Serpone, N.; Meisel, D. *J. Phys. Chem* **1991**, *95*, 5166-5170.

(43) Lawless, D.; Serpone, N.; Meisel, D. *J. Phys. Chem.* **1991**, *95*, 5166-5170.

(44) Serpone, N.; Pelizzetti; Hidaka, H. In *Photocatalytic Purification and Treatment of Water and Air*; Ollis, D. F., Al-Ekabi, H., Eds.; Elsevier: 1993; Vol. 3, p 225-250.

(45) Serpone, N. *Res. Chem. Int.* **1994**, *20*, 953-992.

(46) Fox, M. A.; Dulay, M. T. *Chem. Rev.* **1993**, *93*, 341-357.

(47) Li, X.; Jenks, W. S. *J. Am. Chem. Soc.* **2000**, *122*, 11864-11870.

(48) Noda, H.; OiKawa, K.; Kamada, H. *Bull. Chem. Soc. Jpn.* **1993**, *66*, 455-458.

(49) Turchi, C. S.; Ollis, D. F. *J. Catal.* **1990**, *122*, 178-192.

(50) Li, X.; Cubbage, J. W.; Tetzlaff, T. A.; Jenks, W. S. *J. Org. Chem.* **1999**, *64*, 8509-8524.

(51) Li, X.; Cubbage, J. W.; Jenks, W. S. *J. Org. Chem.* **1999**, *64*, 8525-8536.

(52) Mao, Y.; Schoneich, C.; Asmus, K. D. *J. Phys. Chem.* **1991**, *95*, 80-89.

(53) Carraway, E. R.; Hoffmann, A. J.; Hoffmann, M. R. *Environ. Sci. Technol.* **1994**, *28*, 786-793.

(54) Richard, C. *J. Photochem. Photobiol. A* **1993**, *72*, 179-82.

(55) Emeline, A. V.; Ryabchuk, V.; Serpone, N. *J. Photochem. Photobio. A* **2000**, *133*, 89-97.

(56) Pichat, P.; Herrmann, J.-M. In *Photocatalysis: Fundamentals and Applications*; Serpone, N., Pelizzetti, E., Eds.; John Wiley & Sons: New York, 1989, p 218-206.

(57) Al-Ekabi, H.; Serpone, N.; Pelizzetti, E.; Minero, C.; Fox, M. A.; Draper, R. B. *Langmuir* **1989**, *5*, 250-5.

(58) Matthews, R. W. *J. Catal.* **1988**, *113*, 549.

(59) Stafford, U.; Gray, K. A.; Kamat, P. V.; Varma, A. *Chem. Phys. Lett.* **1993**, *205*, 55-61.

(60) Tunesi, S.; Anderson, M. *J. Phys. Chem.* **1991**, *95*, 3399-3405.

(61) Awatani, T.; Dobson, K. D.; McQuillan, A. J.; Ohtani, B.; Uosaki, K. *Chem. Lett.* **1998**, 849-850.

(62) Li, X.; Cubbage, J. W.; Jenks, W. S. *J. Photochem. Photobio. A* **2001**, *143*, 69-85.

(63) Augustinski, J. *Struct. Bonding* **1988**, *69*, 1.

(64) Terzian, R.; Serpone, N.; Minero, C.; Pelizzetti, E. *J. Catal.* **1991**, *128*, 352-65.

(65) Okamoto, K.; Yamamoto, Y.; Tanaka, H.; Tanaka, M.; Itaya, A. *Bull. Chem. Soc. Jpn.* **1985**, *58*, 2015-2022.

(66) Okamoto, K.; Yamamoto, Y.; Tanaka, H.; Tanaka, M.; Itaya, A. *Bull. Chem. Soc. Jpn.* **1985**, *58*, 2023-2028.

(67) D'Oliveira, J. C.; Guillard, C.; Maillard, C.; Pichat, P. *J. Environ. Sci. Health, Part A* **1993**, *A28*, 941-62.

(68) Serpone, N.; Salinaro, A. *Pure Appl. Chem.* **1999**, *71*, 303-320.

(69) Salinaro, A.; Emeline, A. V.; Zhao, J.; Hidaka, H.; Ryabchuk, V. K.; Serpone, N. *Pure Appl. Chem.* **1999**, *71*, 321-335.

(70) Aguilar, A.; O'Shea, K. E.; Tobien, T.; Asmus, K.-D. *J. Phys. Chem. A* **2001**, *105*, 7834-7839.

(71) San, N.; Hatipoglu, A.; Kocturk, G.; Cinar, Z. *J. Photochem. Photobiol. A.* **2002**, *146*, 189-197.

(72) Matthews, R. W. **1987**, *38*, 405.

(73) Turro, N. J. *Modern Molecular Photochemistry*; University Science Books, 1991.

(74) Fox, M. A. In *Photocatalysis: Fundamentals and Applications*; Serpone, N., Pellizzetti, E., Eds.; John Wiley & Sons: New York, 1989, p 421-455.

(75) Al-Ekabi, H.; Serpone, N. *J. Phys. Chem.* **1988**, *92*, 5726-31.

(76) Balcioglu, A.; Inel, Y. *Turk. J. Chem.* **1993**, *17*, 125-32.

(77) Stafford, U.; Gray, K. A.; Kamat, P. V. *Res. Chem. Intermed.* **1997**, *23*, 355-388.

(78) Stafford, U.; Gray, K. A.; Kamat, P. V. *J. Catal.* **1997**, *167*, 25-32.

(79) Stafford, U.; Gray, K. A.; Kamat, P. V. *Heterog. Chem. Rev.* **1996**, *3*, 77-104.

(80) Stafford, U.; Gray, K. A.; Kamat, P. V. *J. Phys. Chem.* **1994**, *98*, 6343-51.

(81) Stafford, U., University of Notre Dame, 1994.

(82) Mills, A.; Wang, J. *J. Photochem. Photobiol. A. Chemistry* **1998**, *118*, 53-63.

(83) Mills, A.; Davies, R. *J. Photochem. Photobiol. A* **1995**, *85*, 173-8.

(84) Mills, A.; Morris, S.; Davies, R. *J. Photochem. Photobiol. A* **1993**, *70*, 183-91.

(85) Lindner, M.; Theurich, J.; Bahnemann, D. W. *Water Sci. Technol.* **1997**, *35*, 79-86.

(86) Ruppert, G.; Bauer, R.; Heisler, G. *Chemosphere* **1994**, *28*, 1447-54.

(87) Cunningham, J.; Sedlák, P. *J. Photochem. Photobiol. A.* **1994**, *77*, 255-263.

(88) Schmid, S.; Krajnik, P.; Quint, R. M.; Solar, S. *Radiat. Phys. Chem.* **1997**, *50*, 493-502.

(89) Theurich, J.; Lindner, M.; Bahnemann, D. W. *Langmuir* **1996**, *12*, 6368-6376.

(90) Hermann, J.-M.; Matos, J.; Disdier, J.; Guillard, C.; Laine, J.; Malato, S.; Blanco, J. *Catalysis Today* **1999**, *54*, 255-265.

(91) Axelsson, A.-K.; Dunne, L. J. *J. Photochem. Photobiol. A. Chem.* **2001**, *144*, 205-213.

CHAPTER 2. TiO_2 PHOTOCATALYTIC DEGRADATION OF ORGANOPHOSPHONATES

2.1. Introduction

Advanced Oxidation Processes (AOPs) have been used in treating contaminated water. In 1995, Blake listed 300 compounds treated by photocatalytic processes.[1] TiO_2 is the most commonly used catalyst in the photocatalytic oxidation process in waste treatment. The energy needed to activate TiO_2 is about 3.2 eV, which corresponds to near UV radiation of a wavelength of 400 nm or less. Therefore, four to six percent of the solar energy reaching the earth's surface is of the proper wavelengths. When TiO_2 is irradiated, an electron jumps from the valence band to the conduction band, leaving a hole on the valence band. The hole can oxidize water to hydroxyl radical or oxidize an adsorbed organic substrate directly by single electron transfer. In oxygenated aqueous conditions, oxygen can consume the electron, preventing the electron and hole recombination and producing superoxide anion radicals, which further react with water to produce more adsorbed hydroxyl radicals. Degradation of organic compounds can be through the direct hole oxidation or hydroxyl radical reaction, or reaction with superoxide.

Aromatic compounds constitute an important class in water pollution. The photocatalytic degradation of phenol,[2-4] chlorophenol,[5-11] anisole[12] and nitrophenol[13] have been studied. Organophosphorous compounds, mainly from pesticides and nerve agents (see Scheme 2.1), can be harmful for human health.[14]

Scheme 2.1. Structure of pesticide, nerve agents

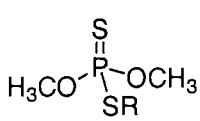

R = $CH(CO_2Et)CH_2CO_2Et$

Malathion

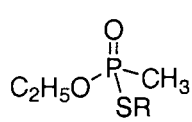

R = $CH_2CH_2N(i\text{-}Pr)_2$

VX

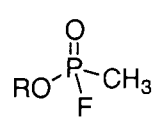

R = *i*-Pr; GB (Sarin)

R = C_6H_{13}; GD (Soman)

Photocatalytic degradation is an effective and clean method for the decomposition of these compounds.[15,16] O'Shea et al. reported that dimethyl methylphosphonate and diethyl methylphosphonate could be completely mineralized to phosphate and carbon dioxide by photoexcited titanium dioxide.[15,16] Further, they proposed two possible pathways to degrade dimethyl methylphosphonate: hydrogen abstraction and addition-elimination as shown in Scheme 2.2.

Scheme 2.2. Proposed hydroxyl radical-mediated degradation mechanisms of dimethyl methylphosphonate

Path A: Hydrogen Abstraction:

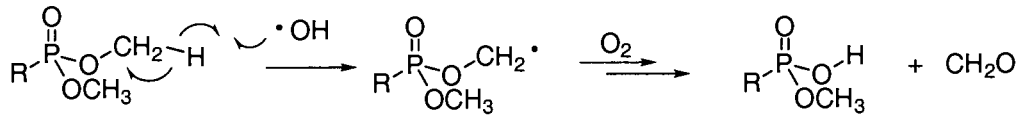

Path B: Addition-Elimination:

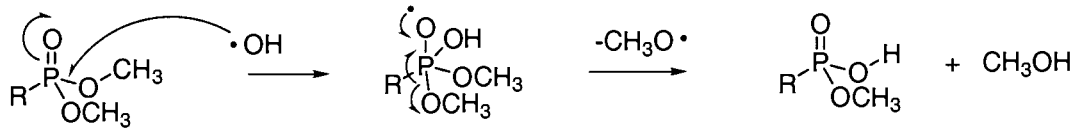

Through analysis of the products of the reaction, they concluded that the hydrogen abstraction mechanism was the predominant reaction pathway, because methanol was not detected, which was proposed to be the product of the addition-elimination pathway. However, it is possible that methanol would have been degraded faster than it was produced.

In contrast, Obee et al.[17] studied the photocatalytic reaction of dimethyl methylphosphonate in the gas-phase on a titanium-coated glass support. They suggested that the degradation of dimethyl methylphosphonate might undergo an addition-elimination mechanism, because they observed methanol, as well as methyl formate, which they supposed was the product of methanol and formic acid. By analogy to reaction of HO• with DMSO that produces methyl radicals after addition to the sulfur center,[18] it is reasonable to anticipate addition of HO• to the phosphorus center of DMPP.

Aguila et al[19] did fundamental mechanistic studies of the radiolytic reactions of dimethyl methylphosphonate and diethyl methylphosphonate. It was found out that hydrated

electrons and superoxide anion radical do not appreciably oxidize the phosphonates, while hydroxyl radical is the main oxidation reagent under radiolysis conditions. They concluded that hydrogen abstraction constituted a major route for the hydroxyl radical reactions based on the intermediate radicals having the ability to easily react with tetranitromethane and the fact that oxygen was critical for the reaction, which is required for hydrogen abstraction mechanism. A sonolysis study by the O'Shea group[16,20] has also suggested that the demethylation goes by an H-abstraction mechanism.

We have used dimethyl phenylphosphonate (DMPP) as a model compound to study the chemistry and mechanism of the photodegradation of organophosphonates by TiO_2. The effects of the initial pH values and the initial concentrations of DMPP on the degradation have been investigated. The reaction is consistent with hydroxyl radical oxidation chemistry and several intermediates have been detected. The phosphoryl substituent on the phenyl ring directs the hydroxyl radical, mainly attacking phenyl at the *meta* position. It is shown that the photodegradation rate was slower for the more electron withdrawing substituent group on the phenyl ring, which might be explained by the electrophilic nature of the hydroxyl radical. d_6-DMPP and ^{18}O labeled-DMPP (Scheme 2.3) have been prepared and used as isotope labeled compounds to explore the demethylation mechanism of the photodegradation, i.e. whether the photocatalytic degradation undergoes path A or path B shown in Scheme 2.2. The results from the degradation of ^{18}O labeled DMPP show that the addition-elimination mechanism is not important.

2.2. Experimental

2.2.1. Materials

Phenylphosphonoyl dichloride, phenylphosphonic acid, dichlorophenylphosphine, pyridine, methanol, methanol-d_4, methylene chloride, tetrahydrofuran (THF), and iodidebenzene were purchased from Aldrich Chemical Company. Phenylphosphonic acid was purified by recrystallization from ethyl acetate. Dried THF was obtained by distillation under argon from THF solution dried by sodium and benzophenone. Dried benzene was obtained by distillation under argon from benzene solution with CaH_2. Other materials were used as

Scheme 2.3. Structures and some abbreviations for the compounds used and prepared in this thesis

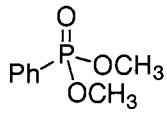

Dimethyl phenylphosphonate (DMPP)

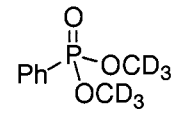

d_6-DMPP

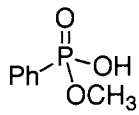

Monomethyl phenylphosphonate (MMPP)

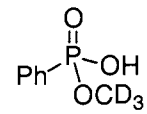

d_3-MMPP

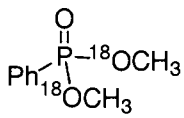

$^{18}O_2$ DMPP

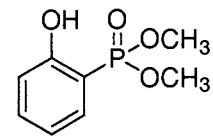

Dimethyl (*o*-hydroxy)-phenylphosphonate (OHP)

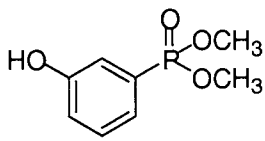

Dimethyl (*m*-hydroxy)-phenylphosphonate (MHP)

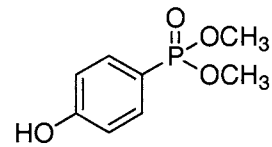

Dimethyl (*p*-hydroxy)-phenylphosphonate (PHP)

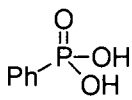

Phenylphosphonic acid

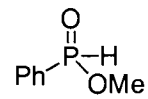

Methyl phenylphosphinate (MP)

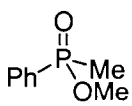

Methyl methyl-phenylphosphinate

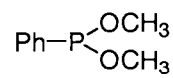

Dimethyl phenylphosphonite

received without further purification. The water was purified by a Millipore Milli-Q UV Plus water purification unit. Titanium dioxide Degussa P25 was used as received.

2.2.2. General Instrumentation

^{1}H and ^{13}C NMR (internal standard TMS), ^{31}P NMR (external standard 85% phosphoric acid) spectral data were obtained on a Varian DRX-400 MHz spectrometer. ^{31}P and ^{13}C NMR spectral data were obtained with ^{1}H decoupling, but ^{31}P coupling remains in the ^{13}C and ^{1}H NMR spectral data. HPLC data were collected with an an HP 1050 liquid chromatograph with diode array UV/VIS absorption detector. LC/MS data were collected on Shimadzu LC/MS-2010 by electrospray ionization (ESI) or atmospheric pressure chemical ionization (APCI). An ODS Hypersil reverse phase column (5 μm, 200 X 2.1 mm, Hewlett Packard) was used. The eluent consisted of a 50% acetonitrile and 50% water mixture. GC data were obtained on HP 5890 gas chromatograph with a 30 m (0.25 mm ID x 0.25 μm) DB-5 column and an FID detector. Mesitylene was used as the internal standard when necessary. The GC/MS data were obtained on a VG Magnum ion trap, a Finnegan TSQ700 triple quadruple mass spectrometer, or a Micromass GCT time-of-flight (TOF) mass spectrometer, as indicated. Centrifugation was accomplished using an Eppendorf 5415 C Microcentrifuge. UV data were obtained on a Shimadzu UV-2101 PC. Flash SiO_2 column chromatography or preparative TLC with 2 mm thickness of silica gel on a 20 cm x 20 cm glass plate was usually used to purify the products.

2.2.3. Preparation

Dimethyl phenylphosphonate (DMPP).[21] To a stirred solution of pyridine (6.57 mL, 0.081 mol) and methanol (3.14 mL, 0.078 mol) in 80 mL of methylene chloride at 0 °C under argon, phenylphosphononic dichloride (5 mL, 0.035 mol) was added dropwise. The mixture was stirred for 5 h at room temperature. The resultant solution was washed with cold water, cold 1 M HCl, cold saturated $NaHCO_3$ solution, and again with cold water, in that order. After drying over anhydrous $MgSO_4$ and subsequent removal of the methylene chloride *in vacuo*, crude DMPP (6.05 g, 93% yield) was obtained. DMPP was purified by SiO_2 column chromatography with ethyl acetate solvent to yield a clear viscous liquid. ^{1}H

NMR (400 MHz, $CDCl_3$) δ 7.73 (2H, dd, J= 13.6, 7.5 Hz), 7.50 (1H, t, J= 7.5 Hz), 7.40 (2H, td, J= 7.5, 4.0 Hz), 3.68 (6H, d, J = 11.2 Hz); ^{13}C NMR (400 MHz, $CDCl_3$) δ 132.7 (d, J = 12 Hz), 131.9 (d, J= 39 Hz), 128.6 (d, J = 60 Hz), 126.9 (d, J = 750 Hz) and 52.7 (d, J= 22 Hz); and ^{31}P NMR (400 MHz, $CDCl_3$) δ 22.2; MS (EI, 70 eV, with TOF ion detector) M/Z (relative intensity), 187 (5), 186 (64), 185 (100), 155 (27), 141 (57), 91 (54), 77 (38).

d_6-Dimethyl phenylphosphonate (d_6-DMPP).[21] The preparation of d_6-DMPP was the same as that of the DMPP except that methanol-d_4 was used instead of methanol. The product was also purified by SiO_2 column chromatography with ethyl acetate solvent. d_6-DMPP: ^1H NMR (400 MHz, $CDCl_3$) δ 7.76 (2H, dd, J = 13.6, 7.5 Hz), 7.53 (1H, t, J = 7.5 Hz), 7.43 (2H, td, J = 7.5, 4.0 Hz); ^{13}C NMR ($CDCl_3$) δ 132.7 (d, J = 12 Hz), 131.9 (d, J = 39 Hz), 128.6 (d, J = 60 Hz), and 126.9 (d, J = 750 Hz); and ^{31}P NMR (400 MHz, $CDCl_3$) δ 22.2; MS (EI, 70 eV, with ion trap) M/Z (relative abundance), 193 (9), 192 (100), 191 (91), 162 (40), 142 (40), 94 (78), 94 (78), 77 (10).

^{18}O-Labeled phenylphosphinic acid.[22] Dichlorophenylphosphine (0.6 mL, 0.0042 mol) in 5 mL THF was added over 15 min to water (0.3 mL; 10% ^{18}O) in 10 mL of THF under Ar. The mixture was stirred for 5 h, followed by removal of the solvent *in vacuo* to produce phenylphosphinic acid, which was recrystallized from ethyl acetate to obtain the product (0.599 g, 96%). ^1H NMR (400 MHz, $CDCl_3$) δ 7.74 (2H, dd, J = 14, 7.5 Hz), 7.69 (1H, t, J = 7.5 Hz), 7.53 (2H, t, J = 7.5 Hz), 7.52 (1H, d, J = 569.6 Hz); ^{31}P NMR (400 MHz, $CDCl_3$) δ 22.8. HPLC/MS (with APCI) 144 (20), 143(100), 142 (90), 91(7), 77(6).

^{18}O-Labeled methyl phenylphosphinate.[23] Cold ethereal diazomethane, prepared immediately before using,[24] was added to the above phenylphosphinic acid (0.599 g) until the yellow color persisted in the solution, and further stirred for 0.5 h at 0 °C. Solvent was removed *in vacuo* to generate reasonably pure methyl phenylphosphinate (0.661 g, 95.8%) that was carried on to the next step. ^1H NMR (400 MHz, $CDCl_3$) δ 3.78 (3H, d, J = 12 Hz), 7.70 (2H, t, J = 10 Hz), 7.59 (1H, d, J = 7.2 Hz), 7.51 (2H), 7.54 (1H, d, J = 566 Hz); ^{31}P NMR (400 MHz, $CDCl_3$) δ 27.8. GC/MS (EI, 70 eV, with ion trap) M/Z 158 (18), 157 (100), 156 (90), 141 (20), 126 (20), 91 (30), 77 (90), 51 (80).

^{18}O-Labeled Dimethyl phenylphosphonite.[25] To the above crude methyl phenylphosphinate (0.661 g, 0.0042 mol), methyl triflormethanesulfonate (0.65 mL, 0.0055 mol) was added dropwise. The reaction mixture was stirred for several minutes at room temperature, then cooled down to about –20 °C. Triethylamine (1.38 mL, 0.0099 mol) in 20 mL dry benzene was added. The mixture was warmed up to ambient temperature, whereby two layers were formed. The top layer contained largely the desired product dimethyl phenylphosphonite. ^{1}H NMR (400 MHz, $CDCl_3$) δ 7.64 -7.58 (2H, m), 7.47-7.38 (3H, m), 3.54 (6H, d, J = 10.4 Hz); ^{31}P NMR (400 MHz, $CDCl_3$) δ 161.3; GC/MS (EI, 70 eV, with ion trap) M/Z (relative abundance), 170 (60), 155 (100), 139 (17), 109 (21), 93 (47), 77 (44), 63 (20), 51 (22); major impurity methyl phenylphosphinate,[23] ^{31}P NMR (400 MHz, $CDCl_3$) δ 27.8, and minor impurity methyl methyl-phenylphosphinate,[26] ^{31}P NMR (400 MHz, $CDCl_3$) δ 44.8. After removal of the solvent, the product mixture (0.524 g) was obtained containing a 2:1:3 mixture of dimethyl phenylphosphonite, methyl phenylphosphinate and methyl methyl-phenylphosphinate. Because dimethyl phenylphosphonite is easily hydrolyzed, impure product was directly used for the next step of synthesis without further purification.

^{18}O-Labeled Dimethyl phenylphosphonates ($^{18}O_2$-DMPP).[21] *t*-Butyl hydroperoxide (1.02 mL, 0.00308 mol) was added to the above product mixture (0.524 g). The mixture was stirred for 0.5 h. The solvent was removed *in vacuo*, and the residue (0.4015 g) was obtained and purified by preparative TLC with ethyl acetate to yield $^{18}O_2$ DMPP (0.159 g, overall 20% from dichlorophenylphosphine). ^{1}H NMR (400 MHz, $CDCl_3$) δ 7.73 (2H, d, J = 7.5 Hz), 7.50 (1H, t, J = 7.5 Hz), 7.40 (2H, td, J = 7.5, 4.0 Hz), 3.68 (6H, d, J = 11.2 Hz); ^{13}C NMR (400 MHz, $CDCl_3$) δ 132.8 (d, J = 12 Hz), 131.9 (d, J = 40 Hz), 128.7 (d, J = 60 Hz), 127.0 (d, J = 750 Hz) and 52.7 (d, J = 22 Hz); ^{31}P NMR($CDCl_3$) δ 22.37; GC/MS (EI, 70 eV, with TOF detector) M/Z (relative abundance), 188 (15),187 (30), 186 (71), 185 (100), 156 (38), 155 (32), 141 (64), 91 (78), 77 (53). Its NMR spectra are shown in the appendix.

Methyl phenylphosphinate.[23] Another simple procedure to synthesize methyl phenylphosphinate starts from methanol when the procedure does not require incorporation of ^{18}O. To a stirred solution of pyridine (3.96 mL, 0.049 mol) and methanol (1.9 mL, 0.0470 mol) in 40 mL of methylene chloride at 0 °C under argon, dichlorophenyl phosphine (2.5 mL,

0.0184 mol) was added dropwise. Thereafter, the mixture was stirred for 5 h at room temperature. The resultant solution was washed with cold water, cold 1 M HCl, cold saturated $NaHCO_3$ solution, and again with cold water, in that order. After drying over anhydrous $MgSO_4$ and subsequent removal of the methylene chloride *in vacuo*, relative pure methyl phenylphosphinate (2.58 g, 90%) was obtained. ^{1}H NMR (400 MHz, $CDCl_3$) δ 3.78 (3H, d, J = 12 Hz), 7.70 (2H, t, J = 10 Hz), 7.59 (1H, d, J = 7.2 Hz), 7.51 (2H), 7.54 (1H, d, J = 566 Hz); ^{31}P NMR (400 MHz, $CDCl_3$) δ 27.8; MS (EI, 70 eV, with ion trap), M/Z 157 (100), 139 (11), 91 (10), 78 (11), 53 (12).

Monomethyl phenylphosphonate (MMPP).[27] To a solution of phenyl phosphonic acid (0.326 g, 0.0020 mol) in dry *N,N*-dimethylformamide (10 mL) at -20 °C controlled by a cooling reagent consisting of the mixture carbon tetrachloride and liquid nitrogen, thionyl chloride (0.18 mL, 0.0024 mol) was added. The mixture was warmed to 0 °C and kept at that temperature for 20 min. Then methanol (0.123 mL, 0.0030 mol) was added. Afterwards, the mixture was warmed to room temperature and stirred overnight. About 20 mL saturated sodium bicarbonate was added to the resultant solution. The aqueous solution was washed with ether (2 x 15 mL), and acidified with concentrated hydrochloric acid (Congo Red). The product was extracted with ethyl acetate. After drying over anhydrous $MgSO_4$ and subsequent removal of ethyl acetate, crude MMPP (0.24 g, yield 70%) was obtained. ^{1}H NMR (400 MHz, $CDCl_3$) δ 7.79 (2H, dd, J = 13.6, 7.8 Hz), 7.51 (1H, t, J = 7.8 Hz), 7.41(2H, td, J = 7.8, 4.4 Hz), 3.67 (3H, d, J = 11.2 Hz); ^{13}C NMR (400 MHz, $CDCl_3$) δ 132.4 (d, J = 11 Hz), 131.5 (d, J = 40 Hz), 128.5 (d, J = 60 Hz), 128.3 (d, J = 770 Hz) and 52.5 (d, J = 22 Hz); ^{31}P NMR (400 MHz, $CDCl_3$) δ 21.5.

MMPP can also be identified and its purity was assessed by LC/MS and GC/MS. A small amount of MMPP needs to be silylated before GC or GC/MS analysis. MMPP (0.001 g) was silylated by treatment with 0.5 mL pyridine, 0.1 mL 1,1,1,3,3,3-hexamethyldisilazane and 0.05 mL chlorotrimethylsilane and removal of pyridinium salts by centrifugation to yield the TMS derivative of MMPP. The crude MMPP was identified by GC/MS. The purity of the product is 81% with DMPP (9%) and phenylphosphonic acid (10%). Further purification was attempted by preparative TLC, but the purity of the compound was not improved. The

mass spectrum of its TMS derivative (EI, 70 eV, with TOF ion detector) M/Z (relative abundance), 244 (5), 229 (100), 199 (10), 153 (17), 121 (11), 89 (13), 75 (13). The UV spectra of MMPP are similar in phosphate buffered solution at pH 7 or without control of the pH, and shown in Figure 2.1.

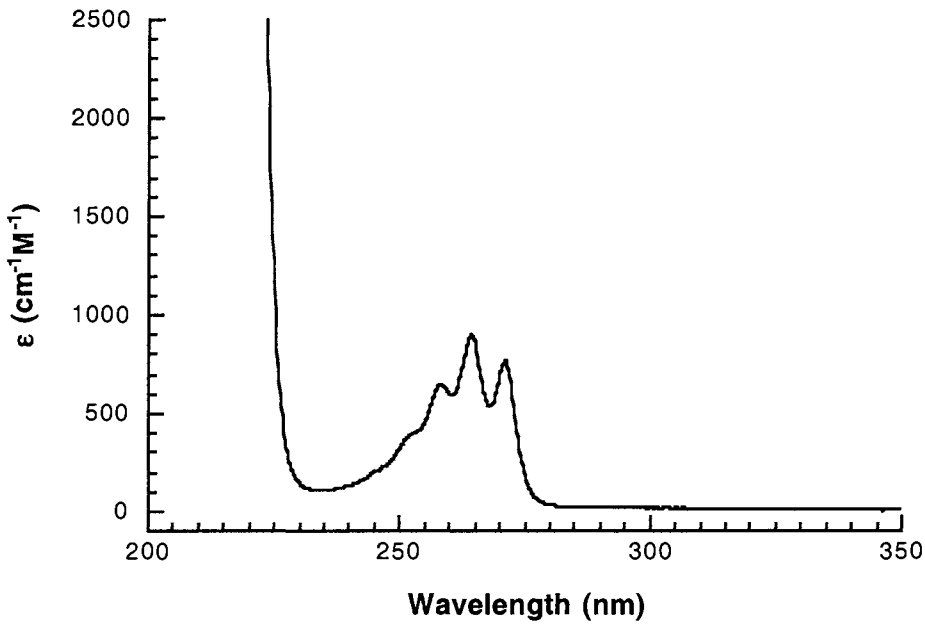

Figure 2.1. The UV spectrum of MMPP at pH = 7.0

d_3-Monomethyl phenylphosphonate (d_3-MMPP).[27] The preparation of d_3-MMPP was the same as the procedure used to prepare the MMPP, except that the methanol was substituted by methanol-d_4. ^{1}H NMR (400 MHz, $CDCl_3$) δ 7.80 (2H, dd, J = 13.6, 7.8 Hz); 7.53 (1H, t, J = 7.8 Hz); 7.43 (2H, td, J = 7.8, 4.4 Hz); ^{13}C NMR (400 MHz, $CDCl_3$) δ 132.5 (d, J = 12 Hz), 131.6 (d, J = 40 Hz), 128.5 (d, J = 60 Hz), and 128.2 (d, J = 770 Hz); ^{31}P NMR (400 MHz, $CDCl_3$) δ 22.0; mass spectrum of its TMS derivative (EI, 70 eV, with TOF ion detector) M/Z (relative intensity) 247 (5), 232 (100), 200 (5), 156 (10), 121 (10).

Dimethyl (*o*-hydroxy)phenyl phosphonate (OHD), dimethyl (*m*-hydroxy)phenyl phosphonate (MHD), and dimethyl (*p*-hydroxy)phenyl phosphonate (PHD).[28] OHD, MHD, PHD were prepared by photolysis of the corresponding aryl iodides in the presence of excess trimethyl phosphite according to the synthetic procedure of Obrycki and Griffin.[28]

The products were purified by preparative TLC (silica gel) with the developing solvents $CH_2Cl_2/CH_3COOC_2H_5$ (6:1), $CH_3COOC_2H_5$, and $CH_3COOC_2H_5$/MeOH (4:1), respectively. OHP: ^{1}H NMR (400 MHz, $CDCl_3$) δ 10.1 (1H, s), 7.45 (1H, t, J = 8.4 Hz), 7.34 (1H, dd, J = 14.4, 7.6 Hz), 6.97 (1H, t, J = 7.6 Hz), 6.92 (1H, t, J = 4.2 Hz), 3.75 (6H, d, J = 11.6 Hz); ^{31}P NMR ($CDCl_3$) δ 25.9; mass spectrum of its TMS derivative (EI, 70 eV, with ion trap) M/Z (relative intensity), 274 (22), 259 (100), 213 (10), 156 (9), 135 (10), 107 (10), 73 (18), 59 (19). MHD: ^{1}H NMR (400 MHz, $CDCl_3$) δ 7.82 (1H, d, J = 15.2 Hz), 7.35 (1H, dd, J = 13.6 Hz), 7.15 (1H, dd, J = 12.8, 7.6 Hz), 7.10 (1H, d, J = 8 Hz), 3.77 (6H, d, J = 11.2 Hz); ^{31}P NMR (400 MHz, $CDCl_3$) δ 22.9; mass spectrum of its TMS derivative (EI, 70 eV, with ion trap) M/Z (relative intensity), 274 (25), 259 (100), 91 (7), 73 (10), 63 (8). PHD: ^{1}H NMR (400 MHz, $CDCl_3$) δ 10.1 (1H s), 7.61 (2H, dd, J = 12.4, 8.4 Hz), 7.01 (2H, d, J = 4.8 Hz), 3.71 (6H, d, J = 11.2 Hz); ^{31}P NMR (400 MHz, $CDCl_3$) δ 24.8; mass spectrum of its TMS derivative (EI, 70 eV, with ion trap) M/Z (relative intensity), 275 (30), 259 (100), 109 (10), 91 (8), 73 (15), 63 (8). The UV spectra of these products are similar in phosphate buffered solutions at pH 7 and without control of the pH. The UV spectra of OHD, MHD, PHD are shown in Figures 2.2.

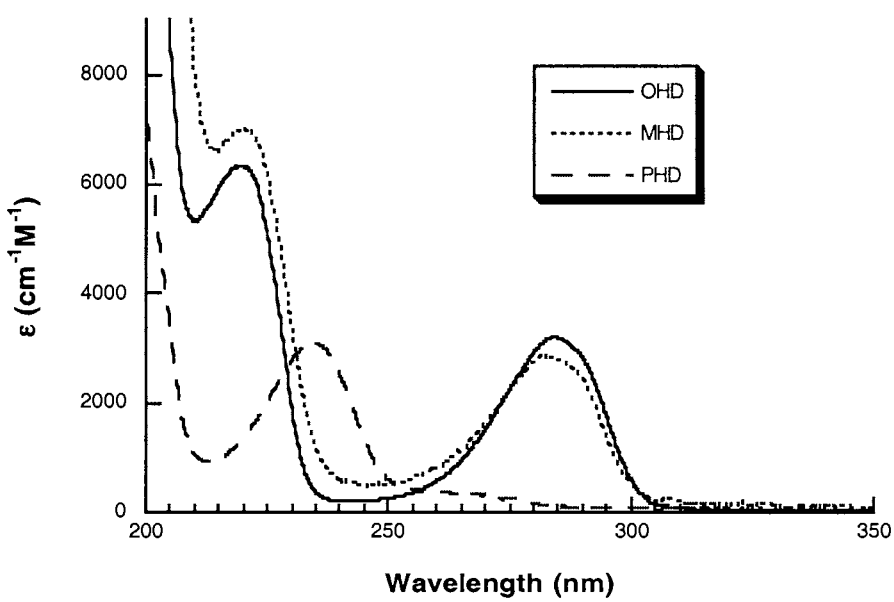

Figure 2.2. The UV spectra of OHD, MHD and PHD at pH = 7.0

2.2.4. Degradation procedures

Typical process for the photodegradation of DMPP. Suspensions were prepared containing 5 mM DMPP and 50 mg TiO_2 in 100 mL water. Due to the small amount of the $^{18}O_2$ DMPP available, 10 mL samples of 5 mM $^{18}O_2$ DMPP and 5 mg TiO_2 were prepared for all of the degradations of $^{18}O_2$ DMPP. The initial pH of the solution was controlled by using HCl (pH = 3), 10 mM phosphate buffer (pH = 7) or 10 mM carbonate buffer (pH = 10). The resultant mixtures were treated in an ultrasonic bath for 5 min to disperse large aggregates. The photodegradation was performed in a Rayonet photochemical reactor with 8 x 4 W "black light" bulbs whose emission is centered at 350 nm. Oxygen was purged through the solution during the reactions. Samples were taken out at desired time intervals and the TiO_2 was separated by centrifugation with an Eppendorf Netheler Hinz 5415 C and filtration through a syringe-mounted 0.2 μm Whatman filter to obtain 5 mL aliquots. The obtained solution can be directly identified by HPLC analysis.

For GC analysis, a different protocol was used. The water was removed *in vacuo* from 5 mL aliquots obtained as above, the samples were silylated by treatment with 0.5 mL pyridine, 0.1 mL 1,1,1,3,3,3-hexamethyldisilazane and 0.05 mL chlorotrimethylsilane. After the pyridinium salts were separated by centrifugation, the samples were analyzed by GC/MS.

H_2O_2 photodegradation of DMPP. Solutions were prepared as above, leaving out the TiO_2. Immediately before photolysis, 1.0 mL of H_2O_2 (30% in water) was added. The degradation was performed in a Rayonet photochemical reactor with 8 x 4 W "black light" bulbs whose emission is centered at 350 nm. After photoreaction, the products were analyzed in the usual way.

Fenton Reaction. Reactions were conducted at room temperature. Normal conditions were 4 mM DMPP, 8 mM $FeSO_4$ and 80 mM H_2O_2 in aqueous solution. The pH was controlled at 7 by using 0.1 M phosphate buffer. After 15 min, the resultant mixture was filtered by 0.2 μm Whatman filter without quenching the reaction to obtain clean solution, followed by analysis in the usual way.

Competition experiment to study the effect of different phenyl substituents. The photodegradation procedure was similar to the general procedure for photodegradation except that a mixture of 2.5 mM DMPP and 2.5 mM anisole or a mixture of 2.5 mM DMPP and 2.5 mM methyl phenylphosphinate was used as the starting materials. At reaction times of 0 h, 1 h, 2 h, 4 h and 6 h, 5 mL aliquots were taken out. After the TiO_2 was removed, 1 mL clear solution was measured out and diluted by adding 3 mL H_2O. Then, 4 mL methylene chloride was used to extract the organic materials. After the organic layer was dried by anhydrous $MgSO_4$, the ratio of the components in the mixture was analyzed by GC.

Study of the isotope effect by a competition reaction. Mixtures with a total concentration of 5 mM, but different ratios of DMPP and d_6-DMPP were degraded in the usual fashion. After photodegradation for 0.5 h and 1 h, the ratio of the concentrations of MMPP and d_3-MMPP was obtained by integrating the base ion peaks in the mass spectra of their TMS derivatives by GC/MS. Degradation reactions under different conditions, such as different initial pH values, H_2O_2 photolysis and a Fenton reaction were investigated.

2.3 Results

2.3.1. Control experiments

Control experiments were performed by eliminating TiO_2, hν or O_2 with all other conditions kept the same under different initial pH values of 3.0, 7.0 and 10.0. Within the time scale of our experiment, the concentration of the DMPP did not change in the absence of TiO_2, hν or O_2. These experimental results indicate that UV light, TiO_2 catalyst and oxygen are all required for the photodegradation of DMPP. If one of these is missing, there is no photodegradation.

2.3.2. Photodegradation of DMPP

Photocatalytic degradation of DMPP in an oxygenated aqueous suspension of TiO_2 with 350 nm excitation was performed. The pH was not regulated. The initial pH is about 6.0. An experiment examining the prolonged photocatalytic degradation of DMPP showed

that DMPP was totally decomposed after 22 hours of photolysis. Several identifiable initial products appeared within a short time (Figure 2.3), which were identified by HPLC, LC/MS, GC/MS and compared to authentic compounds. OHD, MHD and PHD were formed from hydroxylation of the aromatic ring and MMPP were formed by demethylation. No phenol, phenylphosphonic acid or hydroxylated MMPP were observed in the early stages of degradation. Figure 2.4 shows the distribution of these initial products with reaction time. MHD was observed as the major product during the TiO_2 photocatalytic degradation process.

The UV spectra were measured with reaction time. Figure 2.5 shows the change of the UV spectra of the reaction solutions with reaction time. The adsorption around 285 nm apparently belongs to the compounds MHD and OHD. This phenolic absorption reached its maximum when the reaction time was about 10 h. When the reaction time was extended further, the absorption decreased. After 22 h, the characteristic absorption of the benzene ring disappeared and there was no DMPP peak in the GC trace, which indicates total decomposition of the DMPP. However, some absorption still existed, which meant that the intermediates were not completely decomposed to the final products phosphate and carbon dioxide. The total mineralization of DMPP was achieved around 33 h of reaction as determined by UV. The existence of intermediates and slower disappearance of the intermediates than that of the starting materials has usually been observed during the photocatalytic degradation processes. Also, the UV spectra show that the ring opening reaction does not predominate during the first 10 h of reaction, during which demethylation and the hydroxyl radical on the phenyl ring appear to be predominant.

Direct H_2O_2 photolysis in the presence of DMPP has been investigated. After 0.5 h and 1 h, the products were identified by GC/MS and compared with the products of TiO_2 photo degradation. The initial products were the same and the distribution of initial products was similar for both the H_2O_2 photolysis process and the TiO_2 photocatalytic process. After 0.5 h, MHD still appears as the major product (42%) with MMPP (23%), OHP (20%) and PHP (15%) also present; after 1 h, MHD still appears as the major product (53%) with MMPP (20%), OHP (15%) and PHP (12%) also present.

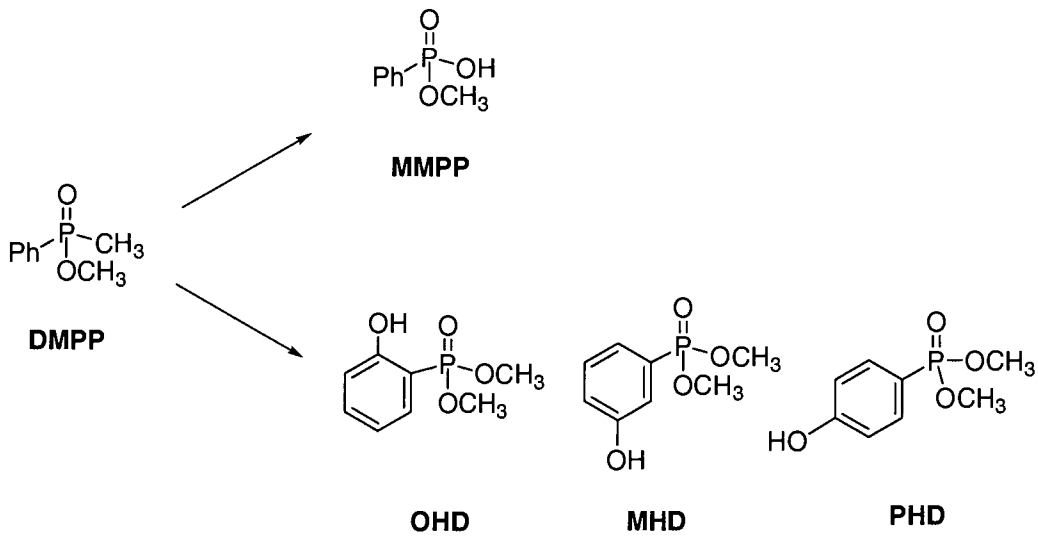

Figure 2.3. The intermediates of the photocatalytic degradation of DMPP

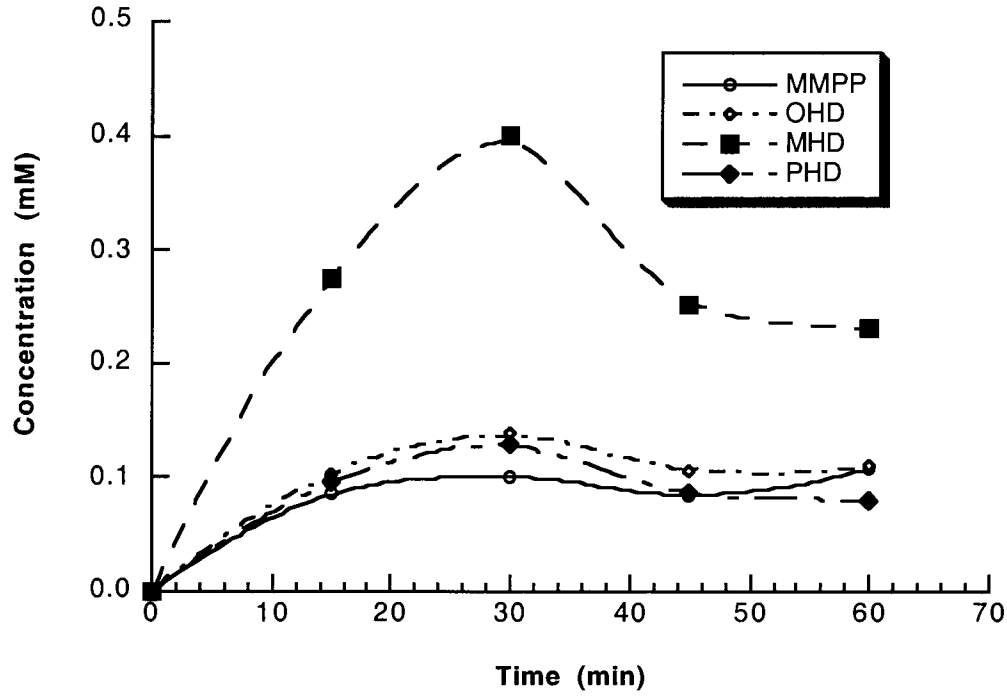

Figure 2.4. The distribution of products as a function of reaction time

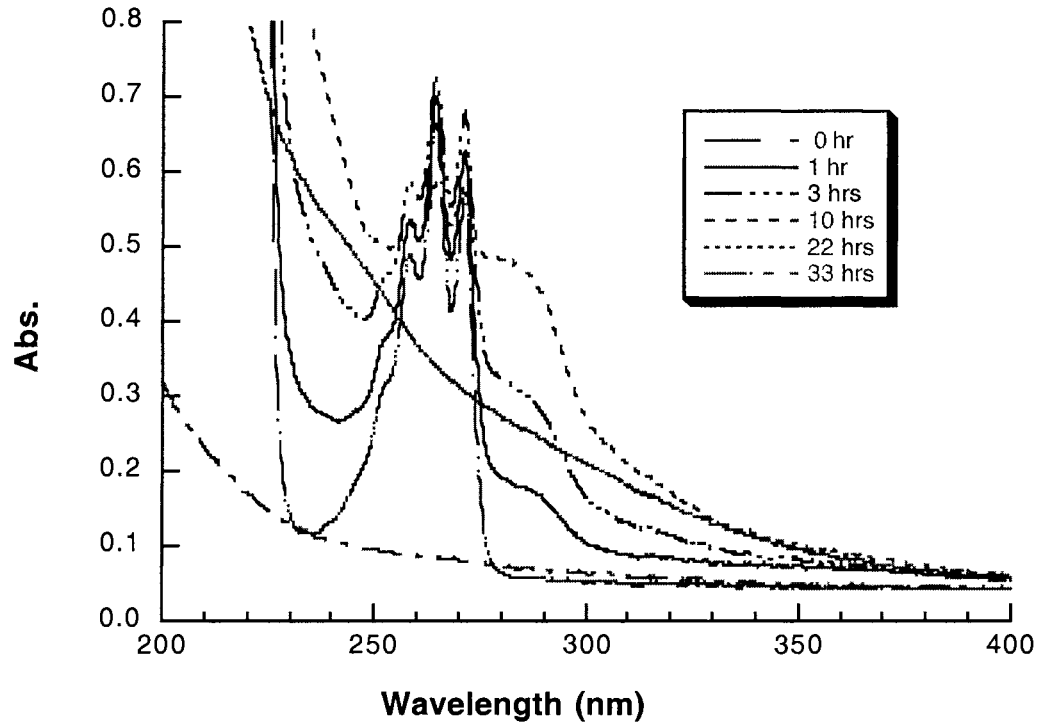

Figure 2.5. The UV spectra of the product solutions with reaction time

2.3.3. Effect of initial pH value on the photocatalytic degradation

The influence of initial pH on the initial rate of the photocatalytic degradation of DMPP has been investigated. The photocatalytic degradation reactions of different samples were performed at different initial pH values of 3.0, 7.0, and 10.0 and the percentage of DMPP remaining in the reaction solutions after 1 h reaction time were identified by GC and shown in Figure 2.6. The higher the pH value of the reaction mixture was, the lower the percentage of DMPP remaining in the reaction mixture after 1 h degradation, which meant that the reaction happened faster at high pH value during the TiO_2 photocatalytic degradation of DMPP.

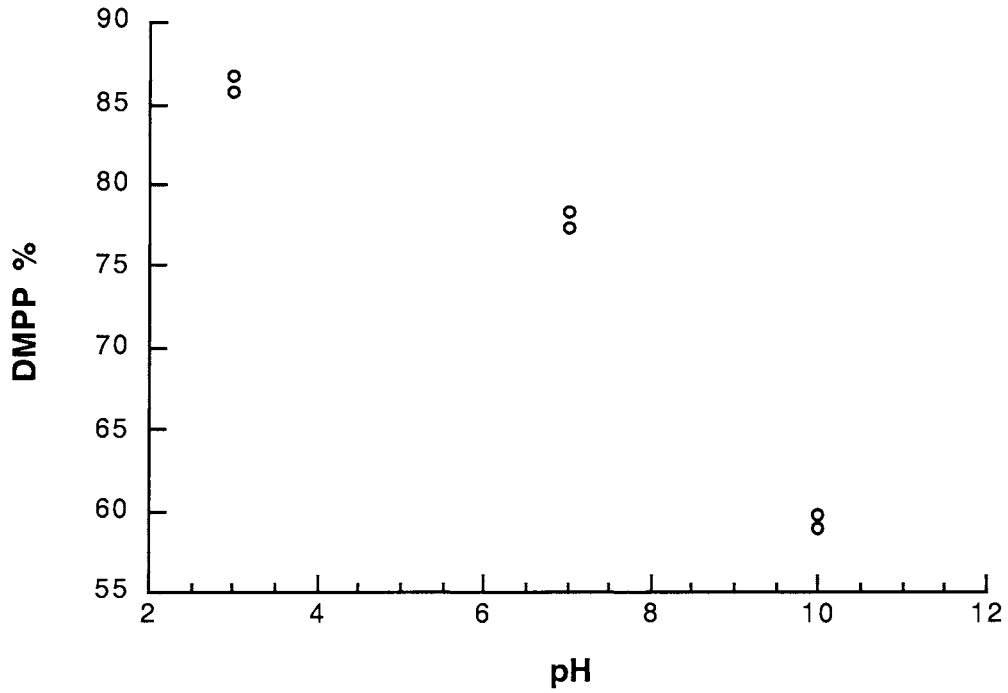

Figure 2.6. The percentage of DMPP remaining under different initial pH conditions after 1 h of degradation

2.3.4. Effect of initial concentration on the photocatalytic degradation

Figure 2.7 shows the oxygen-saturated TiO_2 photodegradation of DMPP at different initial DMPP concentrations of 2.1 mM, 4.6 mM and 9.1 mM without control of pH. The initial pH was 6.0. The decomposition of DMPP fits the exponential equation, which indicates that the degradation of DMPP can be described by a first-order kinetic model. Table 2.1 summarizes the first order rate constants of DMPP at different initial concentrations. However, the apparent degradation rate constant of DMPP is faster at lower initial concentrations of DMPP and slower at higher initial concentrations, which cannot be explained by the simple L-H kinetic model. A similar observation reported by O'Shea et al[16] suggested that strong adsorption of major products may contribute to the reduction in the rates of degradation at higher substrate concentrations. San et al[13] also reported similar results in the photocatalytic degradation of 4-nitrophenol in aqueous TiO_2 suspensions.

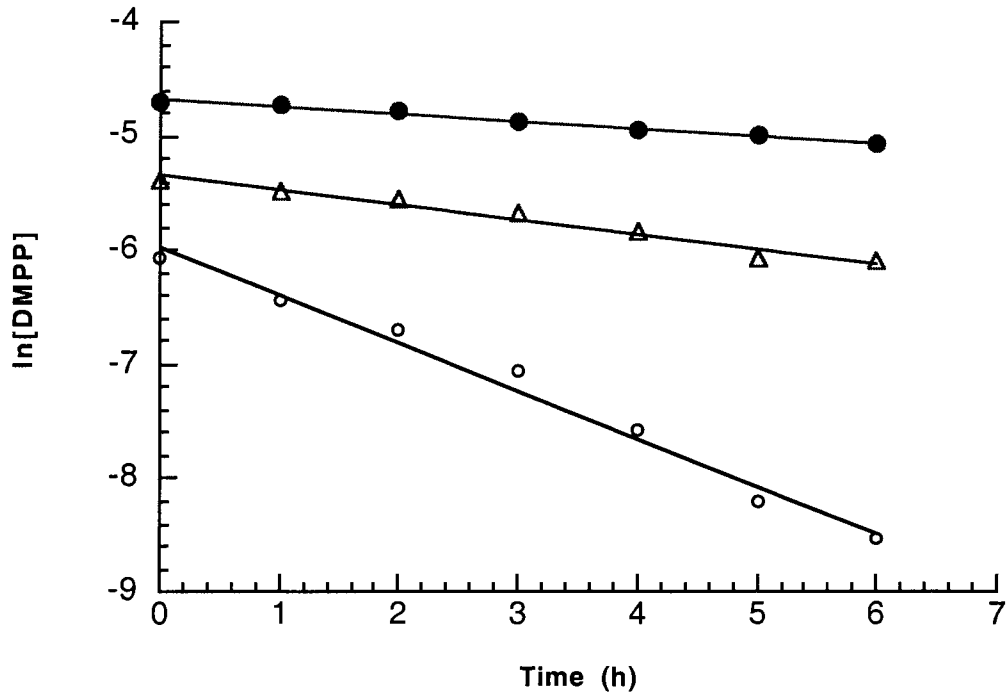

Figure 2.7. Effect of initial concentration on the photodegradation rate of DMPP: (o) 2.1 mM; (Δ) 4.6 mM; (•) 9.1 mM of initial DMPP

Table 2.1. First order rate constants and initial rates for the oxygen-saturated TiO_2 photocatalysis of DMMP as a function of initial concentrations

[DMPP] mM	k ($x10^{-5}$ s^{-1})	Rate (M/s)
2.3	11.65 ± 0.06	2.68×10^{-7}
4.6	3.56 ± 0.28	1.64×10^{-7}
9.1	1.75 ± 0.11	1.59×10^{-7}

2.3.5. Effect of substituents on the phenyl ring on the photocatalytic degradation

The oxidizing species during photodegradation is considered to be the hydroxyl radical or a surface hole. Both of them have electrophilic properties. It is predicted that the

photodegradation happens faster for aromatic compounds with electron-donating substitutents on the phenyl ring than electron withdrawing groups on the phenyl ring when the electrophilic reaction occurs. The following competition reaction was designed to prove this phenomenon.

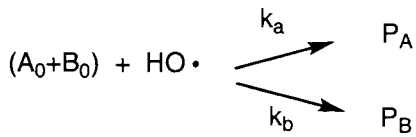

Using a competition reaction can avoid having to use a GC internal standard and can reduce random experimental error. A mixture of 2.5 mM DMPP and 2.5 mM anisole was photodegraded in an oxygenated TiO_2 suspension. A mixture of DMPP and methyl phenylphosphinate was prepared for another experiment. The ratio of the concentrations of the components in the mixtures was analyzed by GC.

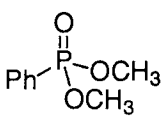

DMPP

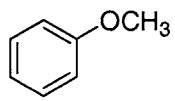

Anisole

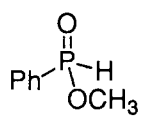

Methyl phenylphosphinate (MP)

A study of the effect of the concentration on the degradation rate already showed that the photocatalytic degradation could be described as a psuedo first order reaction. Assuming kinetic first order behavior suitable for both components in the mixture, the equations for the concentrations of A and B at time t can be described by equations 2.1 and 2.2, where $[A]_t$ and $[B]_t$ are the concentrations of A and B at time t, and $[A]_0$ and $[B]_0$ are the initial concentrations of A and B.

$$[A]_t = [A]_0 e^{-k_1 t} \tag{2.1}$$

$$[B]_t = [B]_0 e^{-k_2 t} \tag{2.2}$$

These equations can be further converted into equations 2.3 - 2.4. The relationship of rate constants for both compounds with the concentrations of the compounds is expressed in equation 2.5 and shown in the Figure 2.8.

$$\frac{[A]_t}{[B]_t} = \frac{[A]_0 e^{-k_1 t}}{[B]_0 e^{-k_2 t}} = \frac{[A]_0}{[B]_0} e^{-(k_1 - k_2)t} \tag{2.3}$$

$$\frac{[A]_t / [A]_0}{[B]_t / [B]_0} = e^{-(k_1 - k_2)t} \tag{2.4}$$

$$\ln\left(\frac{[A]_t / [A]_0}{[B]_t / [B]_0}\right) = -(k_1 - k_2)t \tag{2.5}$$

From the slopes of the lines, the values of ($k_{Anisole}$-k_{DMPP}) and (k_{MP}-k_{DMPP}) are obtained as (1.15 ± 0.12) x10^{-4} s^{-1} and (2.52 ± 0.06) x10^{-5} s^{-1}, respectively. Then, $k_{Anisole}$-k_{MP}, is 9.0 x 10^{-5} s^{-1}. The results show $k_{DMPP} < k_{MP} < k_{Anisole}$, which is consistent with the hypothesis that HO• or h^+ is a possible oxidizing reagent for the photodegradation.

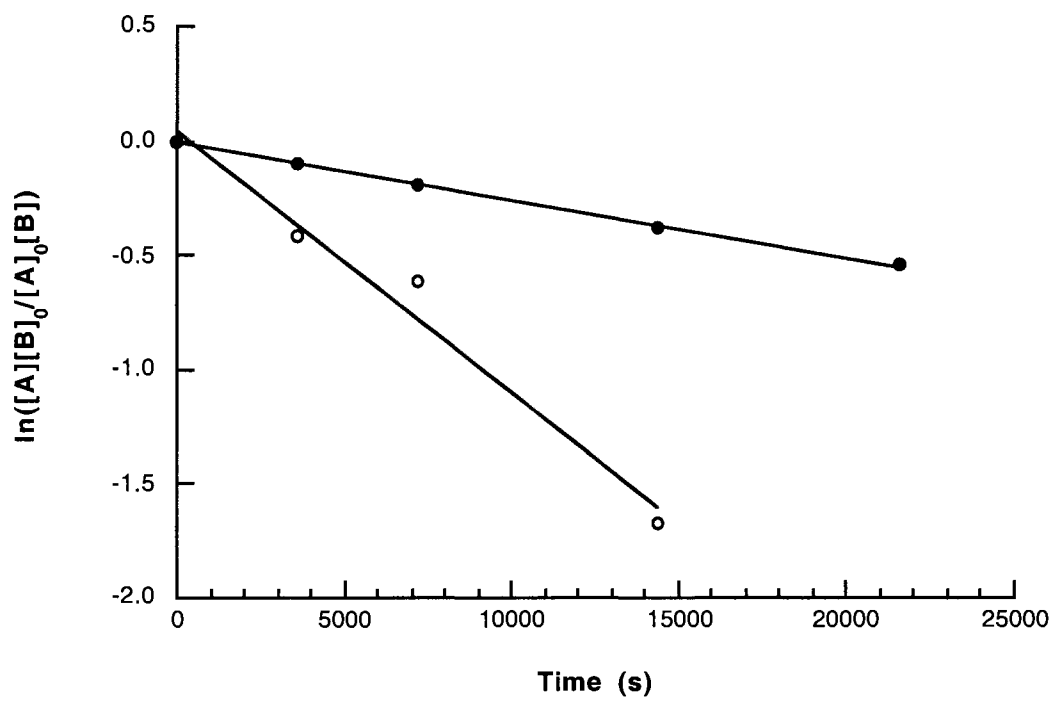

Figure 2.8. The change of ln ([Anisole] $[DMPP]_0$ / [DMPP] $[Anisole]_0$) (o) and ln([MP] $[DMPP]_0$ / [DMPP] $[MP]_0$) (•) with reaction time

2.3.6. Study of the isotope effect by a competition reaction

Competition experiments have been designed to study the photocatalytic degradation mechanism of anisole[12] and trimethyl cyanurate[29] with deuterium labeled compounds. Both of these compounds appeared to degrade by H-abstraction from a methyl and both experiments showed there was a primary isotope effect of k_H/k_D near 3. In this thesis, the competition degradation of DMPP and d_6-DMPP was also designed to investigate a possible kinetic isotope effect. The hypothesis to be tested was that H-abstraction reactions would lead to an isotope-dependent rate of formation of MMPP, assuming that the initial carbon-hydrogen bond breaking step is a rate limiting step. On the other hand, the addition-elimination reactions would lead to an isotope-independent rate of formation of MMPP. The isotope effect can be analyzed by the ratio of the rate constants between the products of MMPP and d_3-MMPP, which can further be expressed by the value of the ratio of their concentrations divided by the ratio of the concentrations of their starting materials based on equation 2.8, obtained as follows:

When the degradation is considered as a pesudo-first order reaction, the following equations 2.6 can be written:

$$\frac{d[MMPP]}{d[d_3-MMPP]} = \frac{k_{MMPP}[DMPP]}{k_{d_3-MMPP}[d_6-DMPP]} \tag{2.6}$$

During the early stage of the degradation, when the concentrations of MMPP and d_3-MMPP are low, and the concentrations of DMPP and d_6-DMPP are high, then $d([MMPP]/[d_6\text{-MMPP}]) \approx [MMPP]/[d_3\text{-MMPP}]$, $[DMPP] \approx [DMPP]_0$, $[d_6\text{-DMPP}] \approx [d_6\text{-DMPP}]_0$. The above equation can be converted into the following equation 2.7:

$$\frac{k_{MMPP}}{k_{d_3-MMPP}} = \frac{[MMPP]}{[d_3-MMPP]} \Big/ \frac{[DMPP]_0}{[d_6-DMPP]_0} \tag{2.7}$$

If it is assumed that the demethylation step is a rate-limiting step, then the equation 2.8 for k_H/k_D can be obtained:

$$\frac{k_H}{k_D} = \frac{[MMPP]}{[d_3 - MMPP]} \Big/ \frac{[DMPP]_0}{[d_6 - DMPP]_0} \tag{2.8}$$

Mixtures with a total concentration of 5 mM, but different ratios of DMPP and d_6-DMPP, were degraded in the usual fashion. Mixtures of 2.5 mM DMPP and 2.5 mM d_6-DMPP were also degraded at different initial pH values in TiO_2 suspensions. The degradation reactions of the mixtures under the direct H_2O_2 photolysis conditions and Fenton conditions were also investigated. After 0.5 h and 1 h (15 min for the Fenton reaction) of reaction time, the concentrations of products of MMPP and d_3-MMPP were analyzed by GC/MS. Due to the similarity of the molecular weight and the physical properties of the TMS derivatives of MMPP and d_3-MMPP, they appeared as a single GC peak. Thus, integration of the base ion peaks in the mass spectra of MMPP and d_3-MMPP were used to determine the ratio of the concentrations of MMPP and d_3-MMPP. The base ion peaks are the peaks of the TMS derivatives of MMPP and d_3-MMPP losing a methyl group, which were the values of 229 and 232, respectively. The values of k_H/k_D for 0.5 h and 1 h reactions were essentially identical. Duplicates of each sample were run, and each run was analyzed 2-4 GC/MS injections.

The results of the competition experiments with different initial pH values and other different conditions are shown in Table 2.2. No isotope effect was observed. This phenomenon may be explained by the addition-elimination mechanism, which can not be taken for granted, because the results were obtained from some premises. For example, there is also no deuterium isotope effect if the hydrogen-abstraction happens after the rate-limiting step. $^{18}O_2$ DMPP must be prepared to further study the degradation mechanism.

Table 2.2. k_H/k_D of the competition reactions under different experimental conditions

Different degradation conditions	k_H/k_D*
$[DMPP]_0/[d6\text{-}DMPP]_0$ =1.5, TiO_2, hν	1.07 ± 0.05
$[DMPP]_0/[d6\text{-}DMPP]_0$ = 0.5, TiO_2, hν	1.07 ± 0.04
$[DMPP]_0/[d6\text{-}DMPP]_0$ =1, pH = 3, TiO_2, hν	1.05 ± 0.08
$[DMPP]_0/[d6\text{-}DMPP]_0$ =1, pH = 7, TiO_2, hν	1.05 ± 0.08
$[DMPP]_0/[d6\text{-}DMPP]_0$ =1, pH =10, TiO_2, hν	1.01 ± 0.04
$[DMPP]_0/[d6\text{-}DMPP]_0$ =1, H_2O_2, hν	0.99 ± 0.05
$[DMPP]_0/[d6\text{-}DMPP]_0$ =1, Fenton	1.01 ± 0.13

* Errors are the standard deviations of multiple experiments

2.3.7. Study of the photocatalytic degradation of ^{18}O-labeled DMPP

The two mechanisms proposed in Scheme 2.2 can be distinguished by the degradation of ^{18}O labeled-DMPP. If the reaction happens by an addition-elimination reaction, a ^{16}OH group will substitute the ^{18}OMe on phosphorus, and thus the ^{18}O enrichment would be expected to decrease in the product MMPP. If the reaction happens by a hydrogen-abstraction reaction mechanism, the hydroxyl radical will attack carbon and the ^{18}O enrichment in DMPP should be the same as that in MMPP because the ^{18}O will be retained in the product.

The ^{18}O-labelled DMPP has been prepared according to the synthetic Scheme 2.4. The advantage of this synthetic method is that the ^{18}O is located on the both methoxy group, and does not local on the phosphoryl group. The difficulties that we met in the synthesis were a tatutomerism in the phosphorus chemistry and the existence of the selective methylation on oxygen and phosphorus. Because of the tatutomerism, after the first hydrolysis step formed trivalent hydroxyl substitution product exists in equilibrium with the tetravalent phosphoryl form (shown in Scheme 2.4 after first synthetic step), which is more stable and has a higher concentration to be detectable spectroscopically.

The methylation problem was solved by sequential methylation with diazomethane and triflate though in modest yield. Dimethyl phenylphosphonite is easily hydrolyzed, so avoiding water is also important in order to achieve a high yield. Because 10% $H_2{}^{18}O$ was used, approximately 20% of molecules have one ^{18}O, 80 % of molecules still have two ^{16}O, only a small amount of molecules have two ^{18}O.

Scheme 2.4. The preparation of ^{18}O labeled dimethyl phenylphosphonate

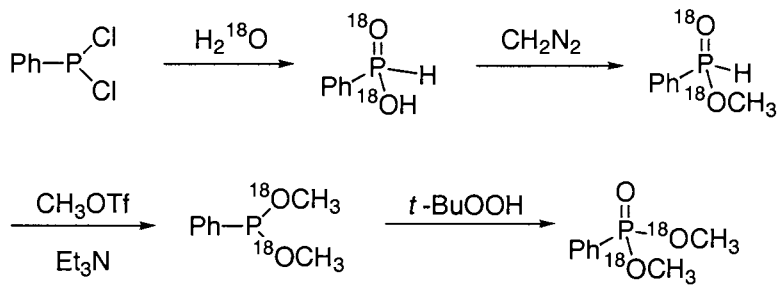

Photocatalytic degradation of $^{18}O_2$ DMPP was carried out. A 10 mL sample of O_2-saturated 5 mM $^{18}O_2$ DMPP and 5 mg TiO_2 was photolyzed at 350 nm. A control experiment without light was investigated. It was found that the ^{18}O enrichment in the DMPP during the control experiment did not change on the time scale of our experiment, showing that

hydrolysis did not play an important role in the production of hydroxylated products. The TiO_2 photocatalytic degradation reactions of ^{18}O-labeled DMPP were studied at different initial pH values and under direct H_2O_2 photolysis. After 0.5 h reaction time, DMPP and the product of MMPP were analyzed by GC/MS (with a TOF ion detector). Two GC/MS runs for every sample and duplicate experiments for the same conditions were performed. The ^{18}O enrichment of DMPP and MMPP was calculated (see Appendix for the calculation). The ^{18}O enrichment in the $^{18}O_2$ DMPP was 9.23 ± 0.06% (standard deviation), which was the average value from many experimental results. Since silylated MMPP easily loses the methyl group during GC/MS analysis, M-15 was the base ion peak for the calculation (Table 2.3). The data show that the ^{18}O enrichment in the starting material DMPP and the ^{18}O enrichment in the products of MMPP are the same within experimental error, which indicates that addition-elimination is not an important mechanism during the degradation process.

Table 2.3. The results of the degradation of ^{18}O labeled DMPP

	^{18}O enrichment in MMPP (%)*
Without control of pH	9.2 ± 0.2
pH = 3, TiO_2, hν	9.4 ± 0.3
pH = 7,TiO_2, hν	9.4 ± 0.1
pH =10, TiO_2, hν	9.3 ± 0.1
H_2O_2, hν	9.0 ± 0.2

* Errors limits are the standard deviations among the measurements. Enrichment of DMPP is 9.23 ± 0.06%.

2.4. Discussion

2.4.1. Effect of initial pH value and concentration

It is shown in Figure 2.6 that the higher the pH value of the reaction mixture is, the faster the DMPP degrades. O'Shea et al.[15] observed the same phenomenon when dimethyl methylphosphonate was used as the substrate. The different degradation rates of DMPP at different pH values may be caused by the different adsorbed concentrations of DMPP on the surface of the catalysts or different hydroxyl radical concentrations. The zero charge for TiO_2 is at pH ~6.6. When the pH of the solution is lower than 6.6, the number of protonated sites on TiO_2 is high and TiO_2 shows overall positive charge. In this case, the weak electrostatic interaction between TiO_2 and DMPP may result in low coverage of DMPP on the catalyst surface and thus a low rate of degradation of DMPP. When the pH of the solution is higher than 6.6, the surface of TiO_2 has a negative charge. Therefore, the electrostatic interaction between TiO_2 particle and DMPP are strong, increasing the concentration of DMPP on the surface. This may rise the degradation rate of the substrate is faster than that of low pH value condition. This hypothesis may be tested by the binding experiment. Another explanation for the increase in the degradation rate with an increase in the initial pH can be attributed to the increased concentration of hydroxyl radicals at the surface of the TiO_2 particles formed by trapping potoexcitated generated hole with higher concentration of HO^- at higher pH value as discussed in Section 1.3.[30]

The photocatalytic degradation rate constant of DMPP is dependent on the initial DMPP concentration. The lower the DMPP concentration is, the faster the rate constant is. The simple L-H kinetic model cannot explain this concentration effect. The strong adsorption of the major products suggested by O'Shea et al[16] may contribute to the reduction in the rates of degradation at higher substrate concentrations. Compared the starting materials of DMPP with the initial products of MMPP, OHD, MHD, PHD, the products are acids and tend to be more strongly adsorbed on the surface of TiO_2 through hydrogen bonding. Adsorption of these products may lead to a reduction in the rates of degradation under the higher concentration. This hypothesis may be tested by experiments to measure the binding constants for the starting material and products.

2.4.2. Degradation consistent with HO• radical chemistry

Several identifiable initial products appeared within a short time (Figures 2.3 and 2.4). The products due to hydroxylation of the aromatic ring and demethylation were observed and the phenol was not observed on the early stages of degradation. The hydroxylated product distribution follows the pattern expected for an electrophilic oxidizing agent. The concentration of MHD is the highest among the four observed products. When the electron withdrawing phosphoryl group is substituted on the phenyl, the *ipso, o,* and *p*-positions become electron poorer than the *m*-position, which results in MHD as the major product. For analogous reasons, because the methoxyl group is an electron donating group, the major primary products of TiO_2 photocatalytic degradation of anisole are *o*-hydroxyanisole, and *p*-hydroxyanisole.[12] This phenomenon is consistent with the idea that $HO•_{ads}$ is the major active species during the photocatalytic degradation of DMPP. The similar product distribution obtained from the hydrogen peroxide photolysis and the the photocatalytic degradation also indicates that hydroxyl radicals are the main oxidizing species for photocatalytic degradation of DMPP.

Figure 2.8 shows the effect of different substituents on the phenyl ring on the degradation rates. Considering the electrophilic $HO•_{ads}$ as the major active species, the rate of anisole should be faster than that of DMPP, since the phosphoryl substitutent on phenyl is an electron-withdrawing group, while the methoxyl substitutent on phenyl is an electron-donating group. The experimental results show that the decomposition of anisole is faster than that of DMPP, which is consistent with the idea that an electrophilic $HO•_{ads}$ is the major active species. Though the substituent on phenyl in methyl phenylphosphinate is also an electron-withdrawing group, there is less oxygen around the phosphorus, which makes the substituent less electron-withdrawing than that of DMPP. Therefore, the reaction rate of methyl phenylphosphinate is faster than that of DMPP and slower than that of the anisole, which is consistent with the experiment. All of the above experiment results are consistent with the idea that an $HO•_{ads}$ radical is the major active species during the TiO_2 photocatalytic degradation of DMPP.

2.4.3. Mechanism study

The reaction mechanism for demethylation (shown in Scheme 2.2) was investigated by the studying the deuterium effect of the photocatalytic degradation of the model compounds of DMPP and d_6-DMPP and the analysis of the ^{18}O enrichment in the starting materials of DMPP and products of MMPP during the degradation of ^{18}O labeled DMPP. If demethylation happens by an H-abstraction mechanism and this step is assume to be the rate-limiting step, a primary deuterium isotope effect will be observed. At the same time, the ^{18}O enrichment in the starting DMPP and MMPP should not be changed since the P-O bond does not break when the H-abstraction mechanism controls the photodegradation of ^{8}O-labeled DMPP. If demethylation happens by an addition-elimination mechanism, no deuterium isotope effect will be observed, and the ^{18}O enrichment in the product of MMPP will be less than that of the starting material of DMPP after the degradation of ^{18}O-labeled DMPP.

The results of a competition experiment involving DMPP and d_6-DMPP in different experiments show that there is no deuterium isotope effect (see Table 2.2). The results of the photocatalytic degradation of ^{18}O-labeled DMPP show that the ^{18}O enrichment in the starting material of DMPP is almost the same as that in the product of MMPP. The experimental results seem to be contradictary to our expectation. The conclusion obtained from the ^{18}O labeled experiment does not depend on any assumption; while the conclusion obtained from the isotope study depends on the assumption of a rate-limiting step. Therefore, the result from degradation of ^{18}O-labeled DMPP is a stronger and more direct evidence for eliminating the addition-elimination mechanism in the photocatalytic degradation of DMPP.

The reason for no deuterium effect may be that $k_H/k_D = 1$. The reaction may be very exothermic or have an early transition state; then k_H/k_D could be around 1. Another explanation may be that a single electron transfer reaction first happens to the substrates. Then the resulting radical cation could lose a proton (or deuterium) after the coming step along the demethylation pathway. It is possible that the demethylation reaction happens after the absorption and adsorption is the rate-limiting step, although this seems to be unlikely, because of the H_2O_2 photolysis results.

In summary, it is reasonable for us to conclude that the addition-elimination mechanism is not possible during the TiO_2 photocatalytic degradation of DMPP.

2.5. Summary

The TiO_2 photocatalytic degradation of DMPP has been studied. The results indicate that DMPP can be completely decomposed in an irradiated TiO_2 aqueous suspension in the presence of oxygen, while the total mineralization of organophosphonates takes longer than the competely decomposition of DMPP. DMPP degrades faster at higher pH values and lower initial concentrations. The photocatalytic degradation reaction can be described by pseudo-first order kinetics. The product distribution, the effect of different substituents on the phenyl ring, the similarity of the initial products obtained from the TiO_2 photocatalytic degradation and H_2O_2 photolysis indicate that the chemistry of photocatalytic degradation of DMPP at the early stages is consistent with hydroxyl radical chemistry. A mechanistic study of the degradation of ^{18}O-labeled DMPP indicates that an addition-elimination mechanism is not likely for the demethylation step.

References

(1) Blake, D. M. "Bibliography of work on the photocatalytic removal of hazardous compounds from water and air, update number 1 to June 1995," available from NTIS, 1995.

(2) Curco, D.; Malato, S.; Blanco, J.; Gimenez, J.; Marco, P. *Sol. Energy* **1996**, *56*, 387-400.

(3) Balcioglu, I. A.; Inel, Y. *J. Environ. Sci. Health, Part A: Environ. Sci. Eng. Toxic Hazard. Subst. Control* **1996**, *A31*, 123-38.

(4) Alemany, L. J.; Banares, M. A.; Pardo, E.; Martin, F.; Galan-Fereres, M.; Blasco, J. M. *J. Adv. Oxid. Technol.* **1998**, *3*, 155-161.

(5) Stafford, U., University of Notre Dame, 1994.

(6) Stafford, U.; Gray, K. A.; Kamat, P. V. *Heterog. Chem. Rev.* **1996**, *3*, 77-104.

(7) Stafford, U.; Gray, K. A.; Kamat, P. V. *Chem. Oxid.* **1997**, *4*, 193-204.

(8) Stafford, U.; Gray, K. A.; Kamat, P. V. *Res. Chem. Intermed.* **1997**, *23*, 355-388.

(9) Stafford, U.; Gray, K. A.; Kamat, P. V. *J. Catal.* **1997**, *167*, 25-32.

(10) Li, X.; Cubbage, J. W.; Tetzlaff, T. A.; Jenks, W. S. *J. Org. Chem.* **1999**, *64*, 8509-8524.

(11) Li, X.; Cubbage, J. W.; Jenks, W. S. *J. Org. Chem.* **1999**, *64*, 8525-8536.

(12) Li, X.; Jenks, W. S. *J. Am. Chem. Soc.* **2000**, *122*, 11864-11870.

(13) San, N.; Hatipoglu, A.; Kocturk, G.; Cinar, Z. *J. Photochem. Photobiol. A.* **2002**, *146*, 189-197.

(14) Yang, Y. C.; Baker, J. A.; Ward, J. R. *Chem. Rev.* **1992**, *92*, 1729.

(15) O'Shea, K. E.; Beightol, S.; Garcia, I.; Aguilar, M.; Kalen, D. V.; Cooper, W. J. *J. Photochem. Photobiol., A* **1997**, *107*, 221-226.

(16) O'Shea, K. E.; Garcia, I.; Aguilar, M. *Res. Chem. Intermed.* **1997**, *23*, 325-339.

(17) Obee, T. N.; Satyapal, S. *J. Photochem. Photobiol. A: Chem.* **1998**, *118*, 45-51.

(18) Dixon, W. T.; Norman, R. O. C.; Buley, A. L. *J. Chem. Soc.* **1964**, 3625-3634.

(19) Aguilar, A.; O'Shea, K. E.; Tobien, T.; Asmus, K.-D. *J. Phys. Chem. A* **2001**, *105*, 7834-7839.

(20) O'Shea, K. E.; Aguila, A.; Vinodgopal, L. K.; Kamat, P. V. *Res. Chem. Intermed.* **1998**, *24*, 695-705.

(21) Siddall, T. H.; Prohaska, C. A. *J. Amer. Chem. Soc.* **1962**, *84*, 3467.

(22) Kay, P. B.; Trippett, S. J. *Chem. Res., Synop.* **1985**, 292-293.

(23) Lei, H.; Stoakes, M. S.; Schwabacher, A. W. *Synthesis* **1992**, *12*, 1255-1260.

(24) Aldrich "Aldrich Technical Bulletin AL-180."

(25) Quin, L. D.; Caster, K. C.; Kisalus, J. C.; Mesch, K. A. *J. Am. Chem. Soc.* **1984**, *106*, 7021-7032.

(26) Szafraniec, L. J.; Szafraniec, L. L.; Aaron, H. S. *J. Org. Chem.* **1982**, *47*, 1936.

(27) Hoffmann, M. *Synthesis* **1986**, 557-559.

(28) Obrycki, R.; Griffin, C. E. *J. Org. Chem.* **1968**, *33*, 632.

(29) Tetzlaff, T. A.; Jenks, W. S. *Org. Lett.* **1999**, *1*, 463-465.

(30) Linsebigler, A. L.; Lu, G.; Yates, J. T., Jr. *Chem. Rev.* **1995**, *95*, 735-758.

APPENDIX

This section will demonstrate how to calculate the relative abundance (setting the major isotope to be 100) for a specific molecular formula. The % ^{18}O enrichment can then be determined for the starting material DMPP and the products of MMPP. All of the data in the calculation were obtained from a Micromass GCT time-of-flight (TOF) mass spectrometry. The relative abundances (setting the major isotope to 100) of the natural isotopes used in the calculation are as follows: $^{2}H = 0.015$, $^{13}C = 1.112$, $^{17}O = 0.038$, $^{18}O = 0.200$, $^{29}Si = 5.063$, $^{30}Si = 3.361$, $^{32}P = 0$.[1]

A.1. The calculation of ^{18}O enrichment of DMPP

The calculation of the ^{18}O enrichment in DMPP is complicated by the fact that there is a significant M-H fragmentation. This means, for instance, that the apparent M^+ peak contains both the parent ion $C_8H_{11}PO_3$ (M = 186) and the deprotonated-but-^{13}C-containing $C_8H_{10}PO_3$. Thus, the contributions by different molecular species to the peaks at 185, 186, 187, and 188 must be deconvoluted.

First, we define the natural abundance factors M* and M** for $C_8H_{11}PO_3$ that contribute to the peaks of 1 and 2 units greater mass than the most abundant isotopes. Setting the major isotope to 100, the factors M* and M** are:

$M^* = 8^{13}C + 11^{2}H + 3^{17}O = 8 \times 1.112 + 11 \times 0.015 + 3 \times 0.038 = 9.175$

$M^{**} = 8 \times 7 \times (^{13}C)^2/200 = 8 \times 7 \times (1.112)^2/200 = 0.346$ (^{18}O ignored)

Second, we must determine the relative contributions to the cluster of M and M-H ions. To a good approximation, this can be done by comparing the relative abundance of the 185 peak to the 186 peak. We call this factor H. The contribution to the 186 peak by $C_8H_{10}PO_3$ with a ^{13}C is small enough that this does not introduce any major error. With this in hand, contributions to 186, 187, and 188 from deprotonated ions can be determined. For example, the relative the contribution to 187 is given by (M*)(H). Once this is accomplished, the excess contribution to 187 is due to ^{18}O in the deprotonated ion, and the excess in 188 is due to ^{18}O in the parent ion. These numbers were self-consistent, but averaged for each MS spectrum. The particular molecular formula(e) which contribute(s) to

the relative abundances of a specific mass peak was identified. The analysis results are shown in Table A.1.

A.1. Relative abundance of the specific molecule for DMPP

m/z	Relative abundance	The molecular formula contributing the relative abundance
185	H	$C_8H_{10}PO_3$
186	$M^*[H]$	$C_8H_{10}PO_3$ with one atom substituted by the corresponding natural isotope atom
	1 by definition	$C_8H_{11}PO_3$
187	$^{18}O[H]$	$C_8H_{10}P^{18}OO_2$
	M^*	$C_8H_{11}PO_3$ with one atom substituted by the corresponding natural isotope atom
	$M^{**}[H]$	$C_8H_{10}PO_3$ with two ^{12}C atoms substituted by two ^{13}C atoms
188	^{18}O	$C_8H_{11}P^{18}OO_2$
	M^{**}	$C_8H_{11}PO_3$ with two ^{12}C atoms substituted by two ^{13}C atoms

The relative abundance of $C_8H_{11}PO_3$, can be obtained by subtracting $M^*[H]$ from the abundance of *m/z* 186. Then, the contributions of parent ions with one or two ^{13}C (M* and M**) atoms may be calculated from the peaks at 187 and 188. The relative abundance of molecule $C_8H_{11}P^{18}OO_2$, can be obtained by subtracting the abundance M** from the 188 peak. The abundance of $C_8H_{10}P^{18}OO_2$ is determined by subtracting the abundance found from M* and M**[H]. These two values are averaged for each determination.

A.2. The calculation of ^{18}O enrichment of MMPP

As mentioned in this thesis, MMPP should be silylated before GC/MS analysis. The TMS derivative of MMPP easily loses a methyl group showing a base ion peak in the mass

spectra. This ion peak has the molecular formula $C_9H_{14}PO_3Si$ (M = 229), which was used in the calculation. By doing this, the calculation can be started from the reliable data and the results of ^{18}O enrichment are not changed

The M +1 and M+2 relative abundances of the natural isotopes of $C_9H_{14}PO_3Si$, defined as M^*, M^{**}, can be calculated as follows (the ^{18}O in natural isotope ignored):

$M^* = 9^{13}C + 14^2H + 3^{17}O + {}^{29}Si = 9 \times 1.112 + 14 \times 0.015 + 3 \times 0.038 + 5.06 = 15.394$

$M^{**} = 9 \times 8 \times (^{13}C)^2/200 + {}^{30}Si = 9 \times 8 \times (1.112)^2/200 + 3.361 = 3.805$

The relative abundances of *m/z* = 229, 230, 231 were obtained from the mass spectra of the TMS derivates of MMPP. The particular molecular formula(e) which contribute(s) to the relative abundances of a specific mass peak were identified. The analysis results are shown in Table A.2. Since there is no M-H peak, the calculation of relative abundance of ^{18}O for MMPP is straightforward. It simply derives from the excess intensity in the 231 peak beyond that expected from the factor M**. For example, the relative abundances of *m/z* = 229, 230, 231 were 100, 21.12, 26.86 from GC/MS. Then $^{18}O[m]$ equals 26.86 - M^{**} = 26.86 - 3.805 = 23.055. The % ^{18}O in each of the two potential oxygen positions in MMPP is thus 9.37.

A.2. Relative abundance of the specific molecule for MMPP

m/z	Relative abundance	The molecular formula contributing the relative abundance
229	[m]	$C_9H_{14}PO_3Si$
230	$M^*[m]$	$C_9H_{14}PO_3Si$ with one atom substituted by the corresponding natural isotope atom
231	$^{18}O[m]$	$C_9H_{14}P^{18}OO_2Si$
	$M^{**}[m]$	$C_9H_{14}PO_3Si$ with two ^{12}C atoms substituted by two ^{13}C atoms, or one ^{28}Si substituted by ^{30}Si

References

(1) Holden, N. E.; Martin, R. L.; Barnes, I. L. *Pure Appl. Chem.* **1983**, *55*, 1119-1136.

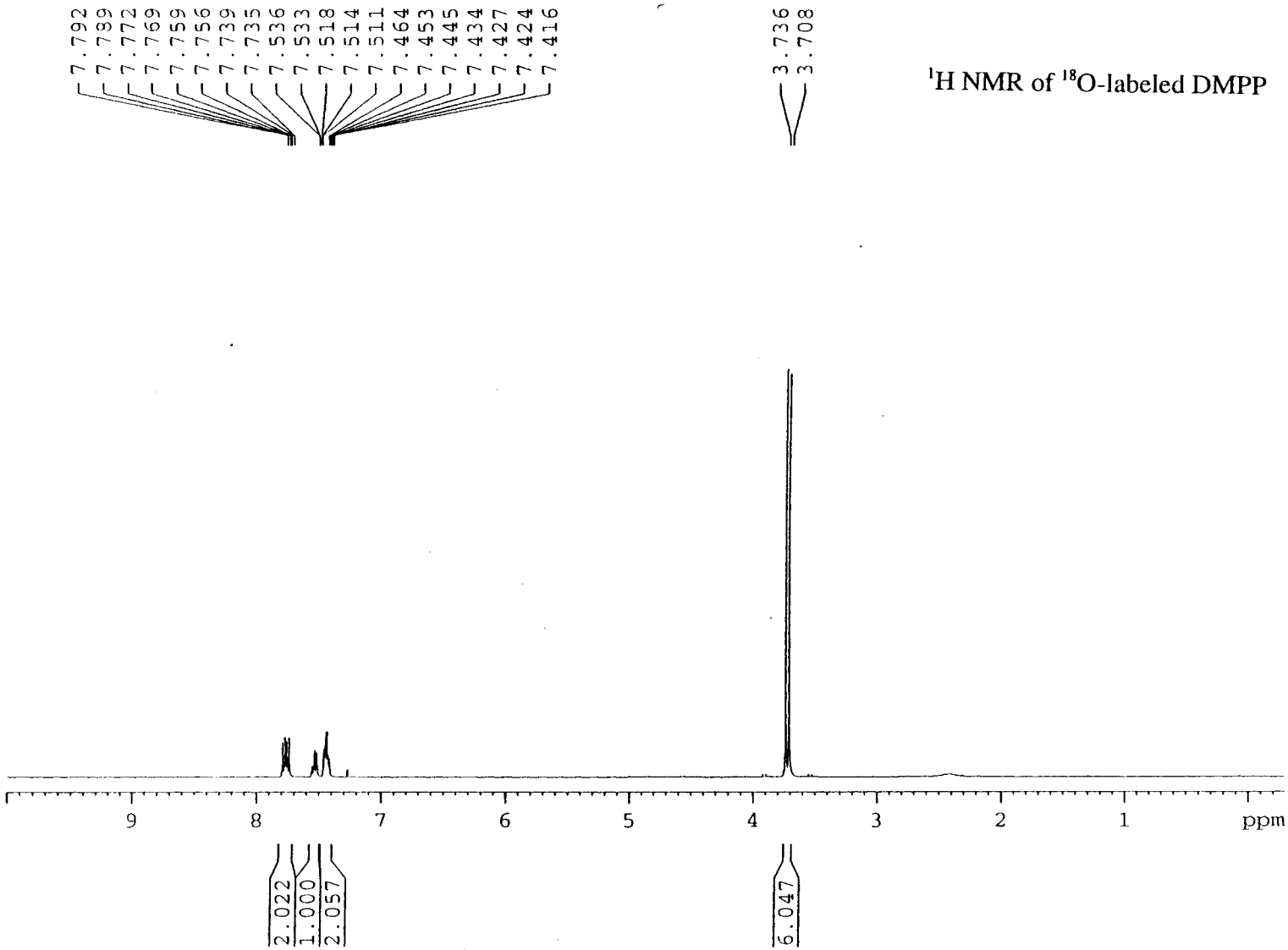

^{1}H NMR of ^{18}O-labeled DMPP

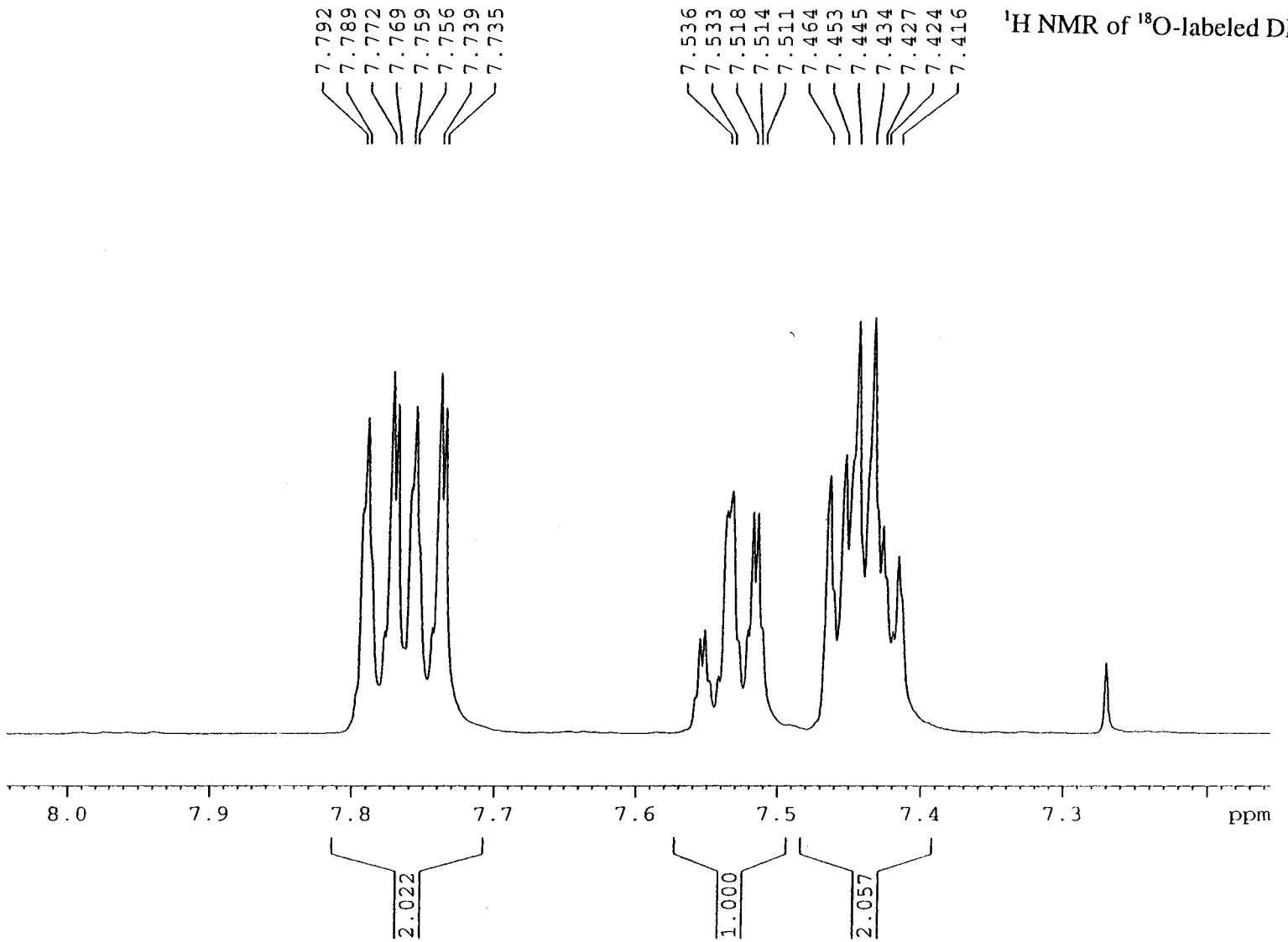

^{1}H NMR of ^{18}O-labeled DMPP

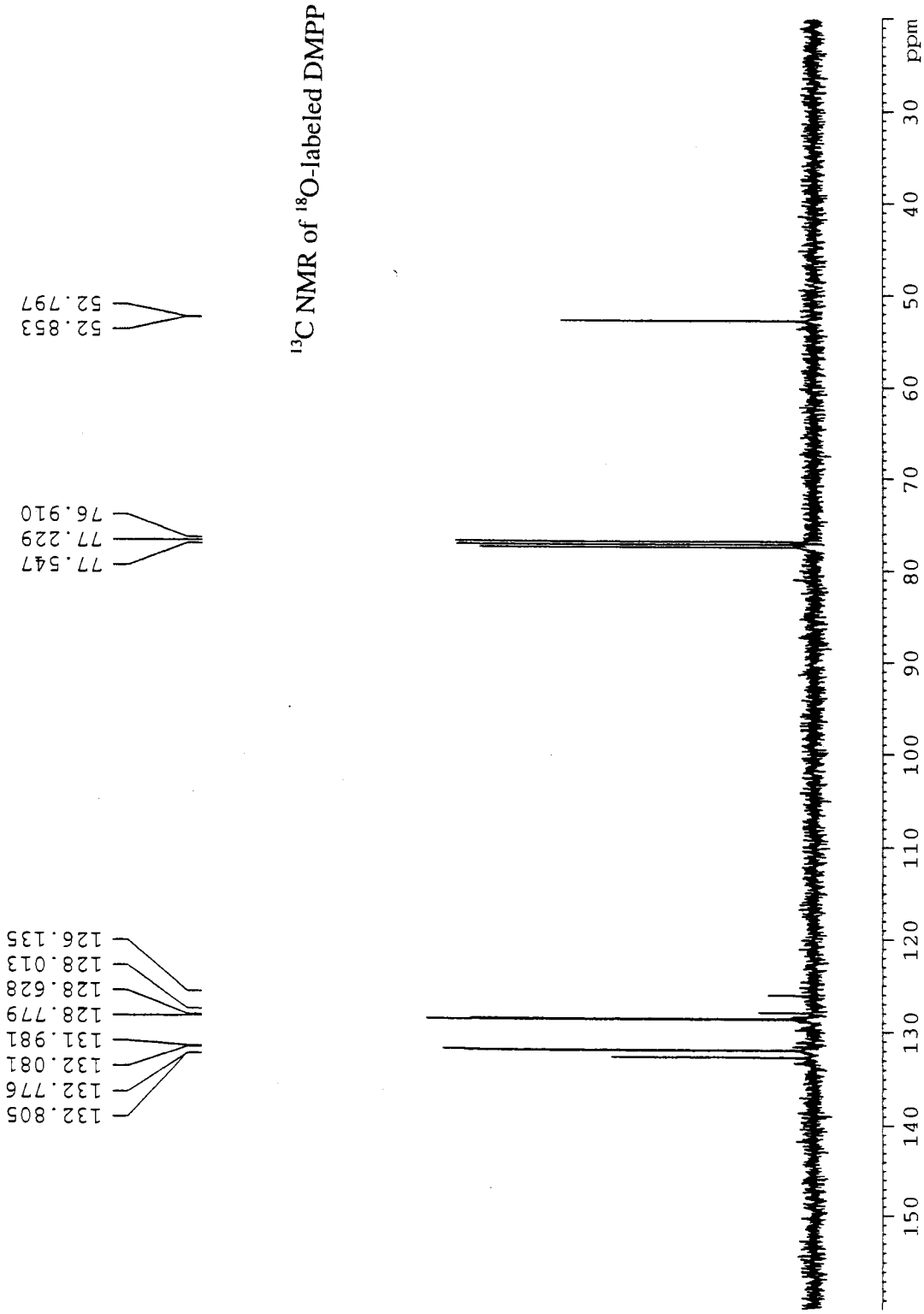
^{13}C NMR of ^{18}O-labeled DMPP
52.797
52.853
77.547
77.229
76.910
132.805
132.776
132.081
131.981
128.779
128.628
128.013
126.135
150
140
130
120
110
100
90
80
70
60
50
40
30
ppm

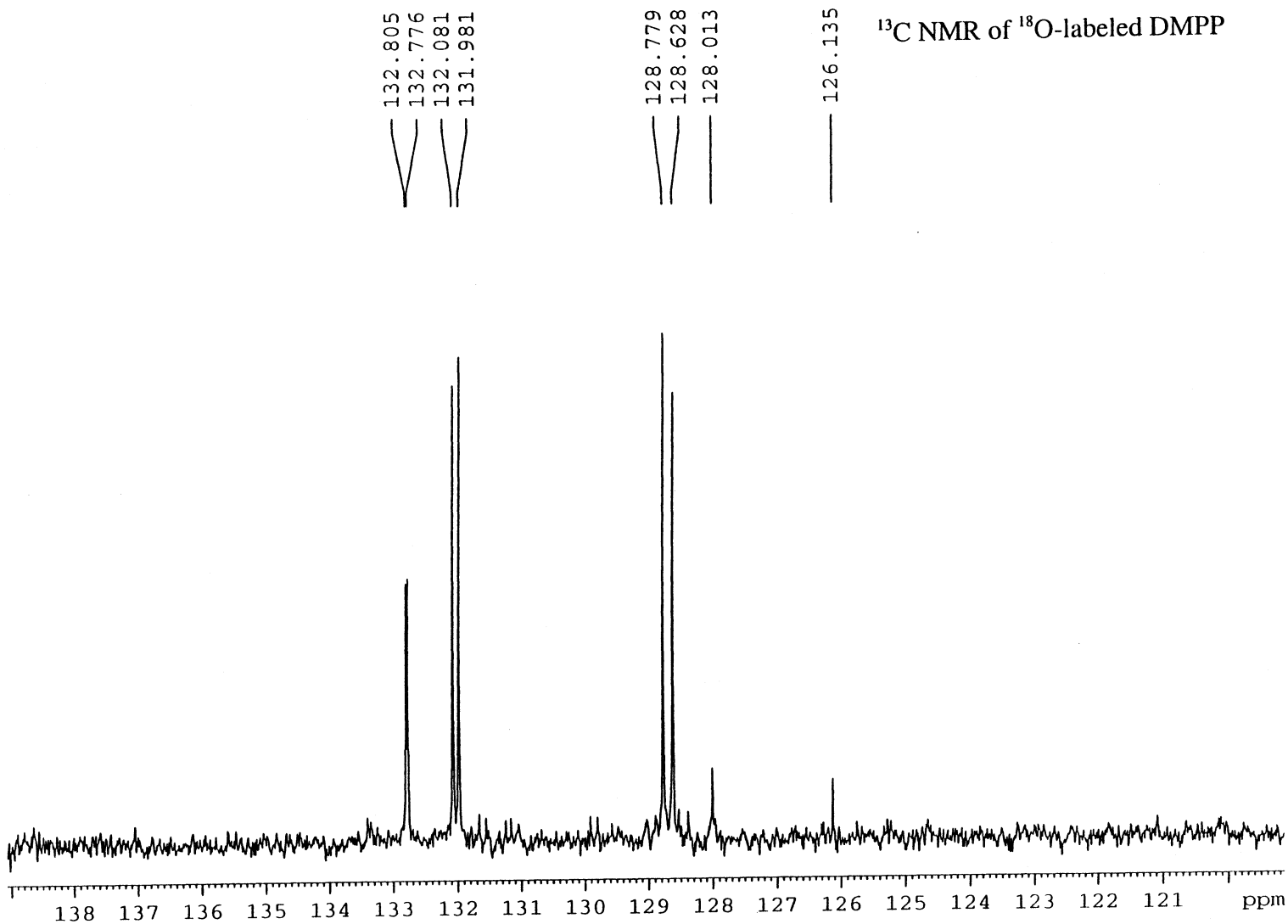

^{13}C NMR of ^{18}O-labeled DMPP

^{31}P NMR of ^{18}O-labeled DMPP

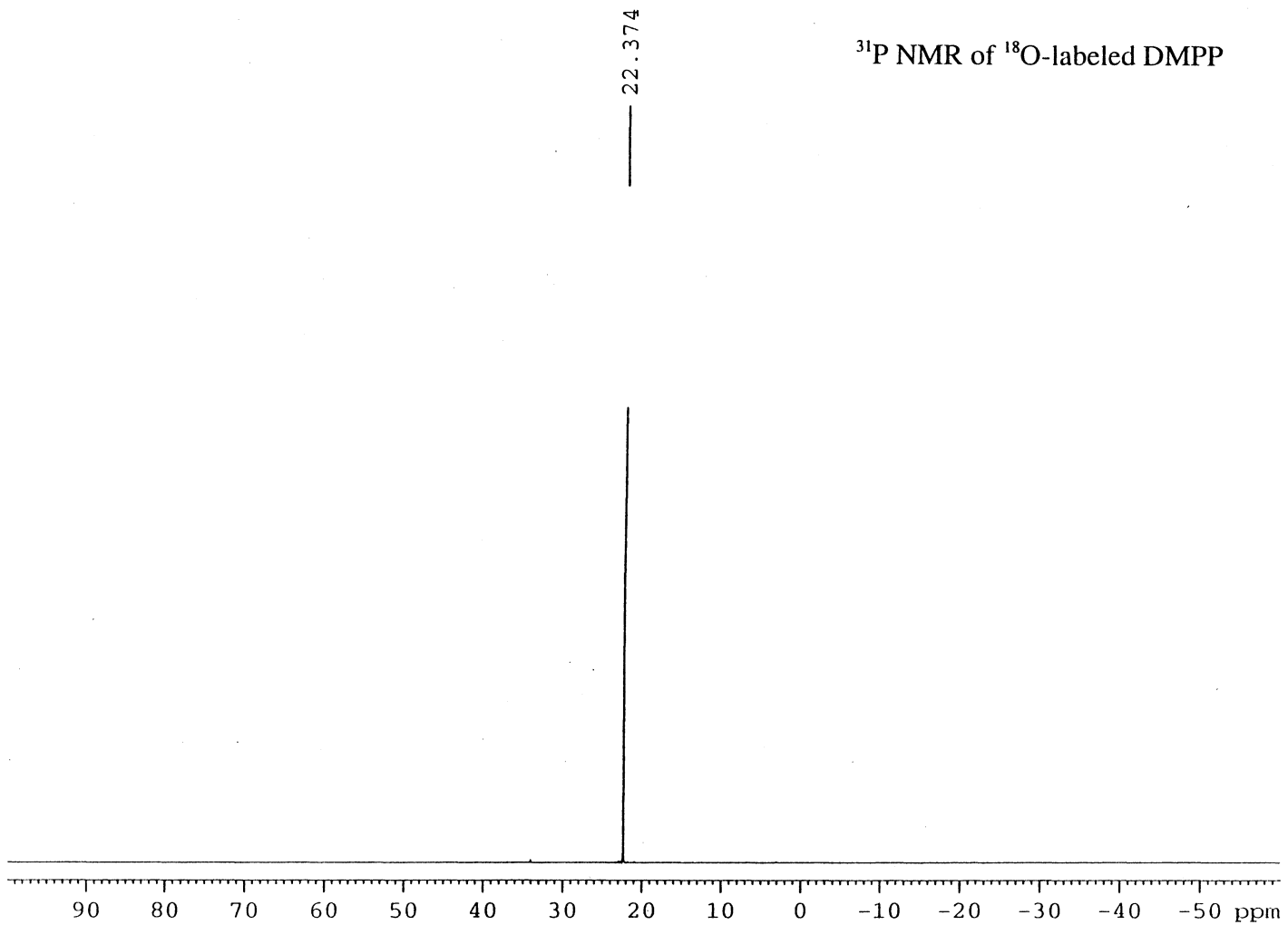

ACKNOWLEDGMENTS

I would like to thank Professor William S. Jenks for his support and guidance in both chemistry and other career-related areas. I appreciate his efforts to lead me to science and his enthusiasm to teach me the knowledge.

I would like to express my thanks to members of the Jenks group, both past and present: Dr. Xiaojing Li, Dr. Woojae Lee, Dr. Jerry Cubbage, Brian Vos, Mrinmoy Nag, Youn-Chul Oh and Ryan McCulla. I would like to thank them for their help and friendship during my stay at Iowa State.

I would like to thank all the people in the instrumental service group, Steve Veysey, Shu Xu, Kamel Harrata and David Scott for teaching me to use GC/MS, LC/MS and NMR.

I would also like to thank my family, my parents, my sister and my husband for their immeasurable support.